



HAL
open science

Novel non-canonical strigolactone analogs highlight selectivity for stimulating germination in two *Phelipanche ramosa* populations

Suzanne Daignan Fornier, Alexandre de Saint Germain, Pascal Retailleau, Jean-Paul Pillot, Quentin Taulera, Lucile Andna, Laurence Miesch, Soizic Rochange, Jean-Bernard Pouvreau, François-Didier Boyer

► To cite this version:

Suzanne Daignan Fornier, Alexandre de Saint Germain, Pascal Retailleau, Jean-Paul Pillot, Quentin Taulera, et al.. Novel non-canonical strigolactone analogs highlight selectivity for stimulating germination in two *Phelipanche ramosa* populations. 2022. hal-03616875

HAL Id: hal-03616875

<https://hal.science/hal-03616875>

Preprint submitted on 23 Mar 2022

HAL is a multi-disciplinary open access archive for the deposit and dissemination of scientific research documents, whether they are published or not. The documents may come from teaching and research institutions in France or abroad, or from public or private research centers.

L'archive ouverte pluridisciplinaire **HAL**, est destinée au dépôt et à la diffusion de documents scientifiques de niveau recherche, publiés ou non, émanant des établissements d'enseignement et de recherche français ou étrangers, des laboratoires publics ou privés.

Novel non-canonical strigolactone analogs highlight selectivity for stimulating germination in two *Phelipanche ramosa* populations

Suzanne Daignan Fornier¹, Alexandre de Saint Germain², Pascal Retailleau¹, Jean-Paul Pillot², Quentin Taulera³, Lucile Andna⁴, Laurence Miesch⁴, Soizic Rochange³, Jean-Bernard Pouvreau⁵, François-Didier Boyer^{1*}

¹ Université Paris-Saclay, CNRS, Institut de Chimie des Substances Naturelles, UPR 2301, 91198, Gif-sur-Yvette, France

² Université Paris-Saclay, INRAE, AgroParisTech, Institut Jean-Pierre Bourgin (IJPB), 78000, Versailles, France

³ Laboratoire de Recherche en Sciences Végétales, Université de Toulouse, CNRS, UPS, Toulouse INP, 31320 Auzeville-Tolosane, France

⁴ Université de Strasbourg, Institut de Chimie, UMR 7177, Équipe Synthèse Organique et Phytochimie, 4 rue Blaise Pascal CS 90032, 67081 Strasbourg Cedex, France

⁵ Nantes Université, CNRS, US2BN, UMR 6286, F-44000 Nantes, France

KEY WORDS: *Phelipanche ramosa*, Parasitic weeds, Germination stimulants, Strigolactones, Synthetic analogs, Structure-activity relationship, Plant hormone, *Pisum sativum*, *Arabidopsis thaliana*, *Rhizophagus irregularis*.

ABSTRACT: Strigolactones (SLs) are plant hormones exuded in the rhizosphere with a signaling role for the development of arbuscular mycorrhizal (AM) fungi and as stimulants of seed germination of the parasitic weeds *Orobanche*, *Phelipanche* and *Striga*, the most threatening weeds of major crops worldwide. *Phelipanche ramosa* is present mainly on rape, hemp and tobacco. *P. ramosa* 2a preferentially attacks hemp while *P. ramosa* 1 attacks rapeseed. The recently isolated Cannalactone **14** from hemp root exudates has been characterized as a non-canonical SL that selectively stimulates the germination of *P. ramosa* 2a seeds in comparison with *P. ramosa* 1. In the present work, we established that (–)-solanacol **5**, a canonical orobanchol-type SL exuded by tobacco and tomato, possesses a remarkable selective germination stimulant activity for *P. ramosa* 2a seeds. We synthesized cannalactone analogs, named (±)-SdL19 and (±)-SdL118 which have an unsaturated acyclic carbon chain with a tertiary hydroxyl group and a methyl or a cyclopropyl group instead of a cyclohexane A-ring, respectively. (±)-SdL analogs are able to selectively stimulate *P. ramosa* 2a revealing that these minimal structural elements are key for this selective bioactivity. In addition, we showed that (±)-SdL19 is able to inhibit shoot branching in *Pisum sativum* and *Arabidopsis thaliana*, and induces hyphal branching in AM fungus *R. irregularis*, like SLs.

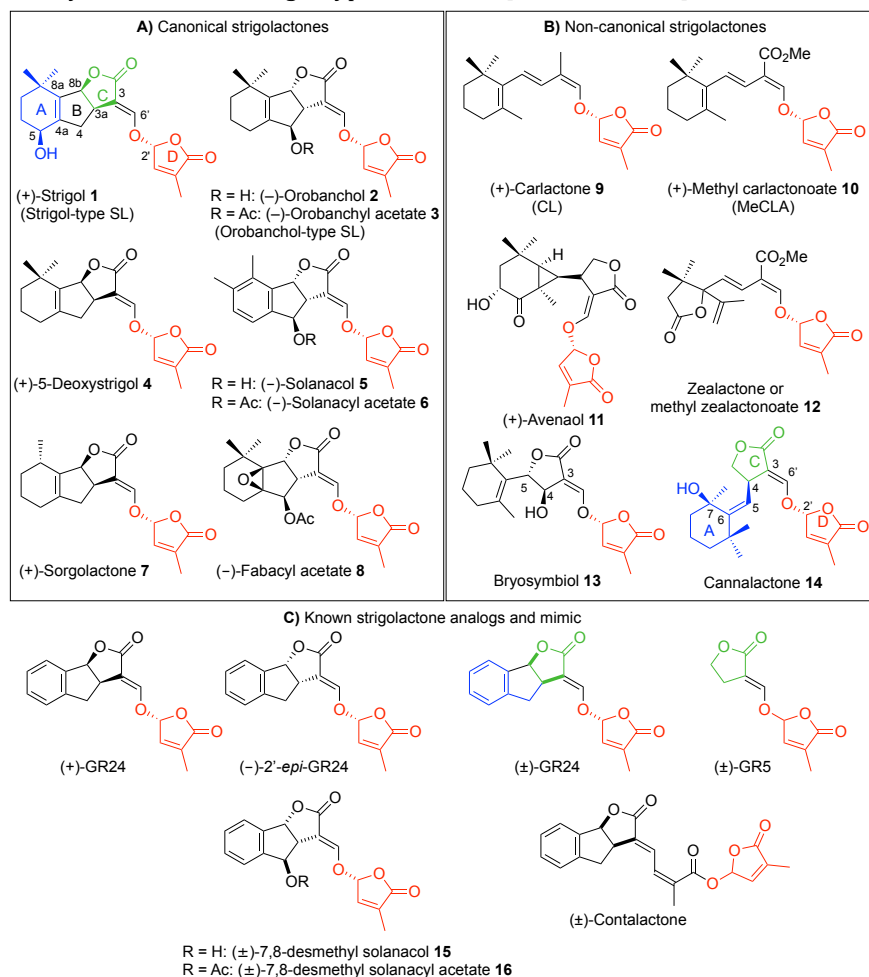
INTRODUCTION

Strigolactones (SLs) are a class of compounds first identified in 1966¹ as stimulants of seed germination of the root parasitic weeds *Orobanche*, *Phelipanche* and *Striga*. More recently, SLs have been discovered as the 9th class of plant hormone that control plant architecture including shoot branching stem secondary growth, plant height, root architecture, and adventitious roots²⁻⁵. They are synthesized in plant roots in trace concentrations, and are partly excreted into the rhizosphere. They belong to the apocarotenoid family (Scheme 1). The structural core of SLs is a tricyclic lactone (ABC part, canonical SLs) or an unclosed BC-ring (non-canonical SLs) connected via an enol ether bridge to an invariant α,β -unsaturated furanone moiety (D ring). All natural SLs have the same *R*-configuration at the C-2' position. Canonical SLs are divided into strigol (**1**)

and orobanchol (**2**) -types corresponding to a β - (e.g., 5-deoxystrigol **4**, sorgolactone **7**) or an α -oriented C-ring (e.g., orobanchyl acetate **3**, solanacol **5**, solanacyl acetate **6**, fabacyl acetate **8**), respectively and with A and B cycles bearing various substituents (Chart 1A)⁶. Non-canonical SLs (e.g., avenaol **11**, zealactone **12**, bryosymbiol **13** and cannalactone **14**) can be structurally more diverse than canonical SLs (Chart 1B). The common biosynthetic precursors for canonical and non-canonical SLs are carlactonoic acid **18** (CLA) and hydroxy-carlactonoic acids (HO-CLAs)⁷⁻⁹ biosynthesized from all-*trans*- β -carotene **17** via carlactone **9** (CL) and hydroxy-carlactones (HO-CLs) (Scheme 1)^{10,11}. In addition, methyl carlactonoate (MeCLA **10**) and HO-MeCLAs^{12,13} have been identified as biosynthetic precursors for numerous non-canonical SLs.

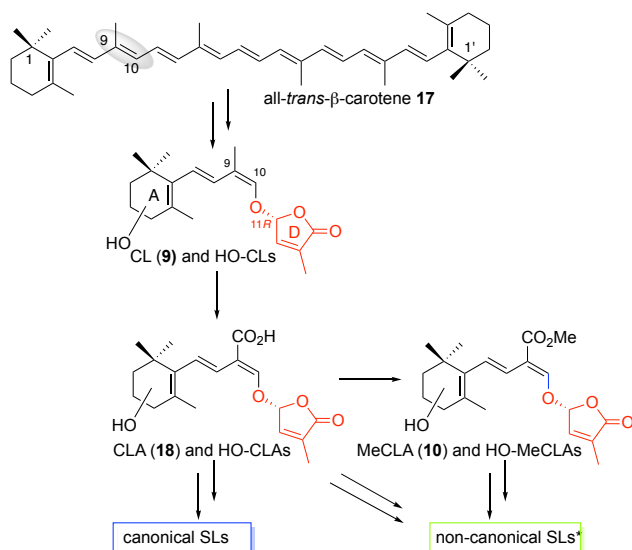
60 To date, more than 23 canonical SLs and more than 10
 61 non-canonical SLs have been identified in plant root exu-
 62 dates and plant tissues¹⁴. Natural SLs are difficult to ob-
 63 tain by organic synthesis due to long multistep
 64 syntheses¹⁵⁻¹⁸. Numerous SL analogs and mimics have
 65 been developed for plant chemical biology^{19,20}. GR24,
 66 invented by Gerald Rosbery, is a canonical strigol-type SL

67 analog with an aromatic A-ring²¹. GR24, in most cases as
 68 racemic mixture, is the worldwide reference compound
 69 (Chart 1C) in all assays investigating the role of SL in bio-
 70 logical processes. The simplified GR-type compound
 71 GR5²¹, possessing only C and D rings (Chart 1C) has been
 72 also developed as a germination stimulant of root parasitic
 73 ic plant seeds and proved later to



74

75 **Chart 1. Natural strigolactones (SLs), canonical (A), non-canonical (B) and artificial SL analogs and mimic (C). For**
 76 **bryosymbiol, the absolute stereochemistry at C-4 and C-5 could be interchangeable²².**



78 **Scheme 1. Strigolactone biosynthetic scheme.** CL=
 79 **carlactone ; CLA = carlactonoic acid ; MeCLA = methyl**
 80 **carlactonate ; SL strigolactone. * Isolated and identi-**
 81 **fied to date.**

82 be bioactive as plant hormone in the control of shoot
 83 branching²³⁻²⁵. More recently, CL²⁶ and MeCLA non-
 84 canonical SL synthetic analogs^{27,28} have been developed to
 85 study the bioactivity of structures close to highly unstable
 86 CL 9 and MeCLA 10¹⁴.

87 The parasitic plants *Orobanche*, *Phelipanche* and *Striga* are
 88 major agricultural pests around the Mediterranean Sea
 89 and in Sub-Saharan Africa, respectively. They tragically
 90 constitute there a major cause of crop damage²⁹ in inten-
 91 sive crop systems that is expected to expand to new terri-
 92 tories in the near future³⁰. They are obligate parasites
 93 producing numerous and extremely small seeds that can
 94 remain viable in soil for decades before germination³¹.

77

95 The induction of germination by host plant SLs is a critical
96 step in the development cycle of these weeds³². SL synthe-
97 sis and signaling are therefore important targets for crop
98 protection^{20,33}.

99 SLs have been shown to play an additional rhizospheric
100 signaling role by stimulating spore germination and hy-
101 phal proliferation of AM fungi^{34,35}. The hypothesis is that
102 plant SLs boost fungal metabolism prior to root infec-
103 tion³⁶. The AM symbiosis arose very early in land plant
104 evolution and is thought to have been instrumental in
105 allowing successful plant conquest of terrestrial environ-
106 ments³⁷. It has been proposed that an ancestral role of SLs
107 was to attract these highly beneficial fungal symbionts²²,
108 root parasitic plants having highjacked this system much
109 later to detect their host²⁵. Biological activities of SLs
110 could be detected at concentrations as low as 10⁻¹³ M on
111 AM fungi, 10⁻¹² M on seeds of parasitic weeds and 10⁻⁸ M
112 on lateral buds as plant hormone.

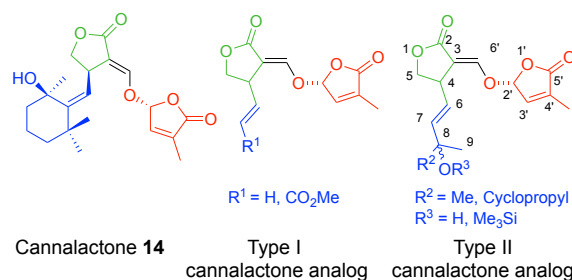
113 *Phelipanche ramosa* seeds recognize allelochemical signals
114 and interact with their hosts depending on their genetic
115 structure as reported recently^{38,39}. Three main genotypic
116 groups were described in European *P. ramosa* populations
117 from the Mediterranean basin. *P. ramosa* of genetic group
118 1 (*P. ramosa* 1) is present exclusively in western France. It
119 parasites essentially oilseed rape but also melon, tobacco,
120 and sunflower. *P. ramosa* 2a attacks preferentially hemp
121 but also tobacco and tomato in France and Italy. *P. ramosa*
122 2b is widespread in Europe and Turkey and attacks
123 mainly tobacco but also various crops like oilseed rape,
124 hemp and tomato. Seed sensitivity to germination stimu-
125 lants as SLs emitted by host plants is proposed as marker
126 of genetic groups. In oilseed rape no SL has been yet iden-
127 tified⁴⁰. Tobacco plants exude canonical strigol-type and
128 orobanchol-type SLs^{41,42} and tomato plants exude oroban-
129 chol-type SLs⁴³. The non-canonical SL cannalactone **14** has
130 been recently characterized from hemp (*Cannabis*
131 *sativa*)⁴⁴. Differential sensitivities to synthetic GR24 enan-
132 tiomers and cannalactone **14** for germination of *P. ramosa*
133 seeds of different genetic groups have been report-
134 ed^{39,44,45}.

135 The SL receptor in vascular plants DWARF14 (D14) has
136 been identified as a member of the superfamily of the α/β -
137 hydrolases^{4,46}. In *Arabidopsis*, a paralog of AtD14,
138 KARRIKIN INSENSITIVE2/HYPOSENSITIVE TO LIGHT
139 (AtKAI2 /AtHTL), has also been described. It encodes a
140 protein that shows a global structure very similar to
141 AtD14 and has conserved the catalytic triad (Ser, His,
142 Asp). AtKAI2 has been shown to regulate *Arabidopsis* seed
143 germination⁴⁷. Interestingly, the *KAI2* gene family has
144 expanded during the evolution of parasitic plant genomes.
145 Some members of these expanded families in witchweeds
146 and broomrapes have evolved the capacity to bind SLs,
147 making them good candidates for SL receptors. Six of the
148 11 *S. hermonthica* KAI2 paralogs, belonging to the diver-
149 gent clade, were identified as highly sensitive to SLs⁴⁸⁻⁵⁰.
150 These results indicated the involvement of one or several
151 α/β -hydrolases in SL perception in parasitic plants. In *P.*
152 *ramosa* 1, among the 5 KAI2 paralogs, we recently estab-
153 lished that PrKAI2d3 encodes a SL receptor which is also
154 able to interact with isothiocyanates (ITCs), other germi-
155 nation stimulants of *P. ramosa* seeds⁵¹.

156 The objective of the present work is to analyze the biolog-
157 ical activity of various cannalactone analogs in compari-
158 son with natural cannalactone **14**, natural SLs and espe-
159 cially SLs produced by tobacco^{41,42} and tomato⁴³ ((-)-
160 orobanchol **2**, (-)-orobanchyl acetate **3**, 5-deoxystrigol **4**,
161 (-)-solanacol **5** and (-)-solanacyl acetate **6**), the SL mimic
162 contalactone⁴⁵ and well-known GR SL analogs. Through a
163 structure-activity relationship (SAR) study, we decipher
164 key minimal structural elements for selective germination
165 activity of *P. ramosa* seeds focused on *P. ramosa* 1 versus
166 2a³⁸ which attack selectively major crops as rapeseed and
167 hemp, respectively. Moreover, we show that these novel
168 non-canonical SL analogs possess hormonal activity in pea
169 and induce hyphal branching in arbuscular mycorrhizal
170 (AM) fungi.

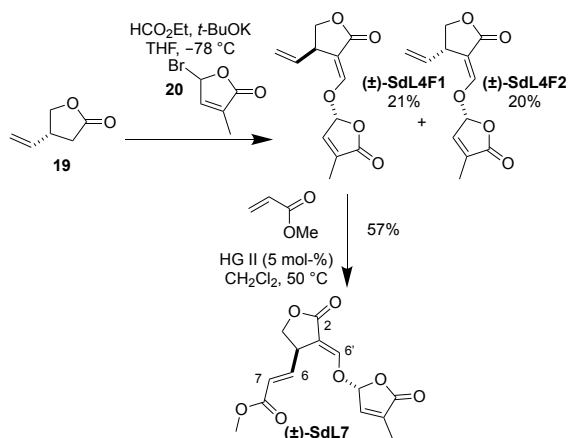
172 RESULT AND DISCUSSION

173 **Synthesis of cannalactone analogs.** We designed two
174 types of cannalactone analogs (Chart 2). Type I possesses
175 an unsaturated acyclic chain instead of the cyclohexane A-
176 ring of cannalactone **14**. Type II bears an unsaturated
177 acyclic carbon chain with a tertiary hydroxyl group and a
178 methyl or a cyclopropyl group (R² group) replacing the
179 cyclohexane A-ring.



181 **Chart 2. Cannalactone analogs Type I and II designed**
182 **in this work. Numbering for cannalactone analogs**
183 **(SdL) and chemicals synthesized here.**

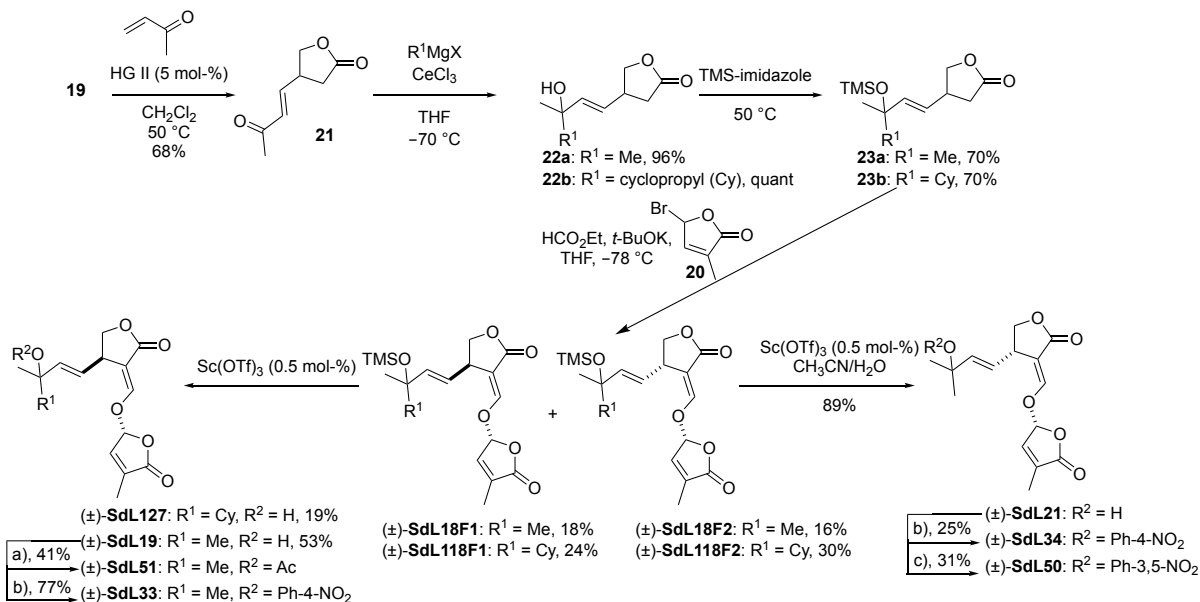
184 The starting material for type I and type II analogs is (\pm)-
185 4-vinyldihydrofuran-2(3*H*)-one **19** or Taniguchi lactone⁵²
186 prepared at multigram-scale from the commercially avail-
187 able *cis*-2-butene-1,4-diol via formation of a ketene acetal
188 and its [3,3]-sigmatropic rearrangement. Formylation of
189 (\pm)-Taniguchi lactone and one-pot coupling with D-Br **20**
190 at -78 °C led to the formation of diastereomers Type-I
191 cannalactone analogs (\pm)-SdL4F1 and (\pm)-SdL4F2 easily
192 separable by silica gel chromatography in 41% overall
193 yield (Scheme 2). SdL7, another Type-I cannalactone ana-
194 log was obtained by cross metathesis (CM) of (\pm)-SdL4F1
195 with a large excess of methyl acrylate at 50 °C with Hov-
196 eyda-Grubbs II (HG II) initiator in 57% yield. The *E*-
197 geometry of the α,β -unsaturated ester group and the *E*-
198 geometry of the enol function in SdL7 were proven by
199 NMR analysis (³J_{H6-H7} = 15.5 Hz, ³J_{C2-H6'} = 2.0 Hz).



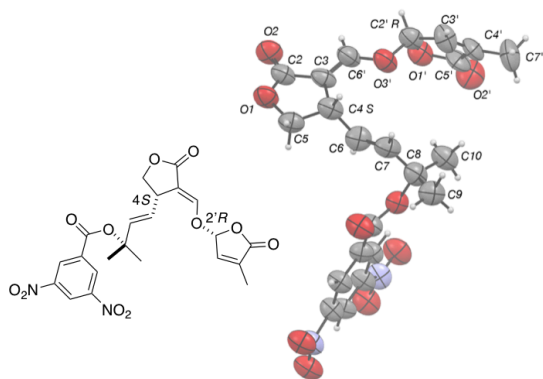
Scheme 2. Preparation of Type-I cannalactone analogs: (±)-SdL4F1, (±)-SdL4F2 and (±)-SdL7.

Preparation of Type-II analogs with R¹ = methyl or cyclopropyl group involved the sequence detailed in Scheme 3. Taniguchi lactone **19** was engaged in CM with butane-3-one in presence of HG II and afforded enone **21** in 68% yield. The selective addition of methyl and cyclopropyl group on the ketone group of enone **21** was accomplished using Grignard reagents with cerium(III) chloride leading to alcohol **22a** and **22b** in near quantitative yields^{53,54}. Cerium(III) chloride plays an important role in increasing the nucleophilicity and decreasing the basicity of the Grignard

reagents. The direct formylation on alcohols **22a,b** was unsuccessful. However, silylation of alcohols **22a,b** in neat trimethylsilyl imidazole furnished protected derivatives **23a,b** in 70% yield, which led by formylation and coupling with D-Br **20** to a separable mixture of diastereomers in moderate yields (34-54%) ((±)-SdL18F1/(±)-SdL18F2, (±)-SdL118F1/(±)-SdL118F2). A mild deprotection of separated silylated derivatives ((±)-SdL18F1, (±)-SdL18F2) with catalytic Lewis acid (Sc(OTf)₃) and H₂O⁵⁵ led to both alcohols (±)-SdL19 and (±)-SdL21 in non optimized 53 and 89% yields, respectively. However, these conditions for the silylated cyclopropyl derivative (±)-SdL118F1 were inefficient but the targeted alcohol (±)-SdL127 was produced with scandium(III) triflate and Ac₂O⁵⁶ in poor 19% yield and without detection of the acetylated product. Tertiary alcohols (±)-SdL19 and (±)-SdL21 were acylated by standard conditions to furnish acetylated derivative (±)-SdL51 and 4-nitrobenzoates (±)-SdL51 and (±)-SdL50. In addition, formation of 3,5-nitrobenzoate (±)-SdL50 from (±)-SdL21 furnished a crystalline compound whose X-ray diffraction properties were sufficiently exploited to establish unambiguously the relative configurations of stereogenic centers C2' and C4 of (±)-SdL50 as 2'R and 4S, respectively (Figure 1) and by consequence the relative configurations of stereogenic centers for the other SdL analogs. With these putative SL analogs in our hands, their biological activity was studied.



Scheme 3. Preparation of Type-II cannalactone analogs (±)-SdL18F1, (±)-SdL18F2, (±)-SdL19, (±)-SdL21, (±)-SdL33, (±)-SdL34, (±)-SdL50, (±)-SdL51, (±)-SdL118 and (±)-SdL127. a) Ac₂O, 4-DMAP, pyridine, rt ; b) ClCO-Ph-4-NO₂, 4-DMAP, pyridine, 40 °C ; c) ClCO-Ph-3,5-NO₂, 4-DMAP, pyridine, 40 °C.



245

246 Figure 1. ORTEP view of the asymmetric unit of (±)-SdL50
 247 (solvent molecule omitted) with selected atom numbering.
 248 Ellipsoids are represented with 30% of probability.

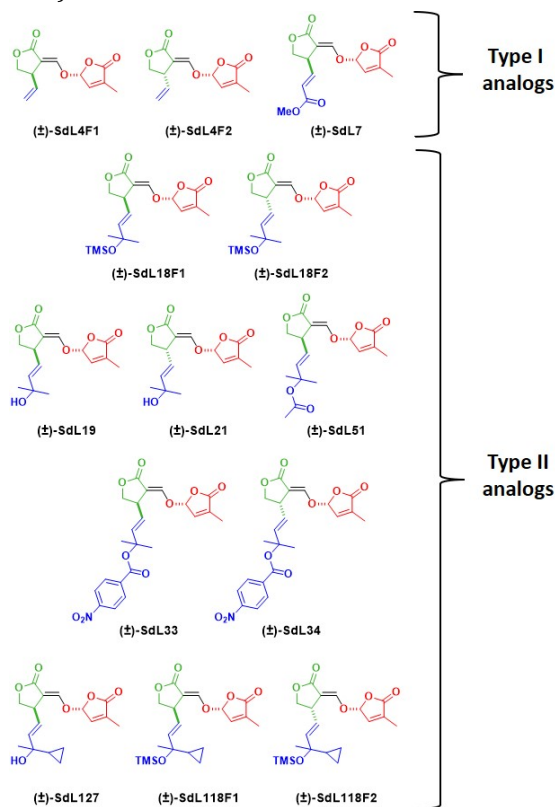
249 **Most SdL derivatives possess similar bioactivity and**
 250 **selectivity as cannalactone toward *Phelipanche ramosa***
 251 **1 versus 2a.** The germination stimulant activities of
 252 SdL analogs on *P. ramosa* 1 and 2a seeds were determined
 253 and compared to (±)-GR24, (±)-GR5 and natural cannalactone
 254 **14** by measuring the maximum of germination
 255 stimulant activity as well as half maximal effective concentrations
 256 (EC_{50}) using a concentration range from 10^{-13} to
 257 10^{-6} mol.L⁻¹ (Chart 3, Figure 2A)⁵⁷. Germination stimulant
 258 activities of all SdL analogs and the putative cannalactone
 259 biosynthetic precursor, (±)-MeCLA, reached the maximum
 260 induced by (±)-GR24 which makes them germination
 261 stimulants as expected for SL analogues (Figure S1A). We
 262 compared the bioactivities of these chemicals based on
 263 EC_{50} values.

264 We previously reported that cannalactone **14**, a non-
 265 canonical SL, possesses a stronger germination stimulation
 266 activity on *P. ramosa* 2a than on *P. ramosa* 1. On contrary,
 267 (±)-GR24, an artificial canonical SL possesses a
 268 stronger germination stimulation activity on *P. ramosa* 1
 269 rather than on *P. ramosa* 2a⁴⁴. These results led us to propose
 270 that *P. ramosa* 1 could be more sensitive to canonical
 271 SLs and *P. ramosa* 2a to non-canonical SLs. To illustrate
 272 the selectivity of seed germination between *P. ramosa* 1
 273 and *P. ramosa* 2a, the ratio of EC_{50} (*P. ramosa* 1/ *P. ramosa*
 274 2a) (r_{EC50}) of each molecule was calculated (Figure 2B); for
 275 example, r_{EC50} ((±)-GR24) = 0.014 and r_{EC50} (**14**) = 410.

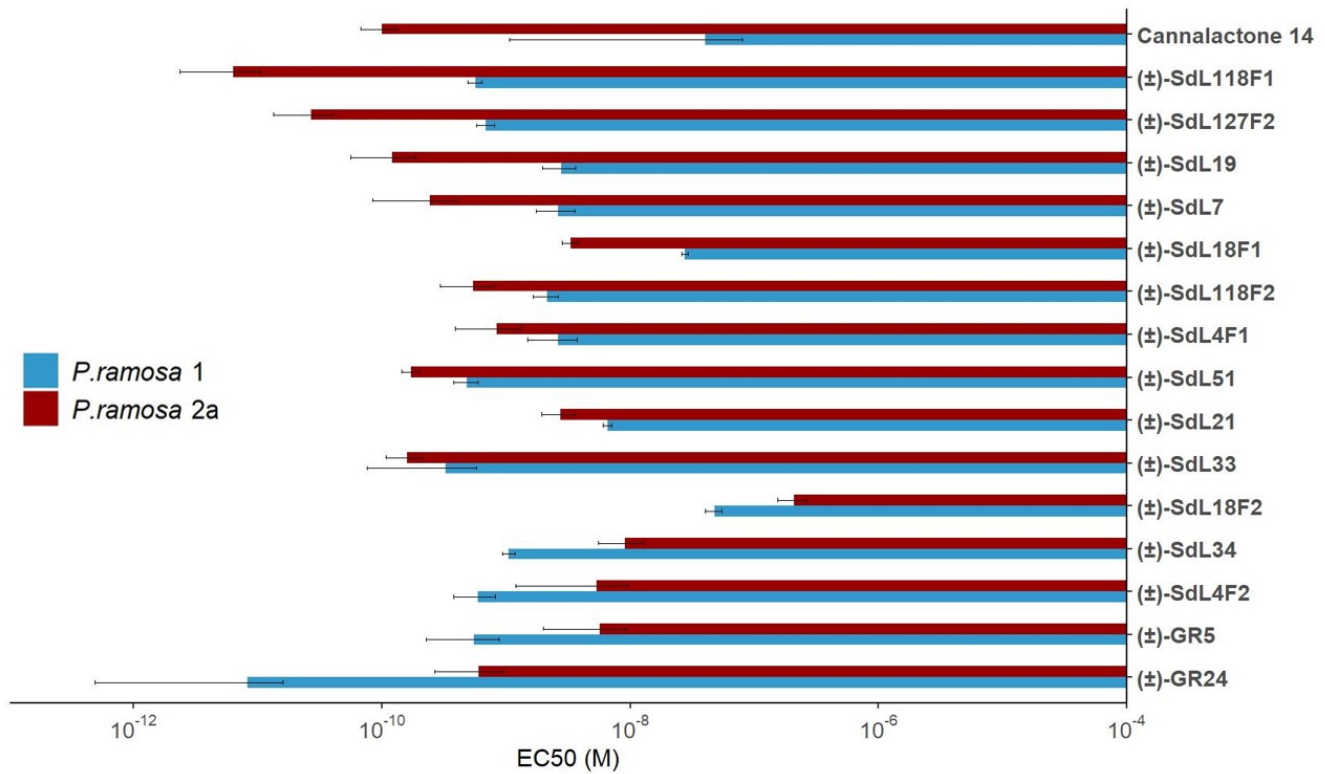
276 We studied a set of various canonical SLs belonging to
 277 strigol- ((±)-**1**, (±)-**4**, (±)-**7**) and orobanchol-types ((±)-**2**,
 278 (±)-**3**, (-)-**5**, (-)-**6**, (±)-**8**) and (±)-contalactone (Chart 1),⁴⁵
 279 a recent SL mimic discovered during the preparation of
 280 (±)-GR24. All canonical SLs (**1-4**, **7-8**) and (±)-
 281 contalactone⁴⁵ were found less active than (±)-GR24, (+)-
 282 GR24 and (-)-2'-*epi*-GR24,⁴⁵ possessing stereochemistries
 283 found in natural canonical SLs (strigol-type and orobanchol-
 284 type, respectively). Their r_{EC50} (< 1) reflect selectivity
 285 for *P. ramosa* 1, except for the cases of (-)-solanacol **5** and
 286 (-)-solanacyl acetate **6** where high germination activity
 287 and selectivity for *P. ramosa* 2a were recorded (r_{EC50} ((-)-
 288 **5**) = 164) (Figure 3, Figure S1B). Though high germination
 289 activities were observed with (-)-solanacyl acetate **6** and

290 7,8-desmethyl solanacol derivatives **15** and **16**, selectivity
 291 was reduced, highlighting the importance of the hydroxyl
 292 group but also the methyl group on the A aromatic ring for
 293 selectivity. High levels of (-)-solanacol **5** and (-)-solanacyl
 294 acetate **6** were detected in tobacco root exudates⁴¹ and in
 295 tomato root extracts⁴³. To note, tobacco and tomato plants
 296 are also hosts for *P. ramosa* 2a^{38,39}, in accordance with the
 297 sensitivity of *P. ramosa* 2a seeds to (-)-solanacol **5** and
 298 (-)-solanacyl acetate **6** shown here.

299 We studied the germination stimulation activities of the
 300 SL biosynthetic intermediates (Scheme 1). For all-*trans*- β -
 301 carotene **17**, a SL biosynthetic precursor without D-ring,
 302 no germination was recorded, demonstrating that this
 303 compound is not bioactive and/or that no enzyme of the
 304 SL biosynthesis pathway was sufficiently present in plant
 305 parasitic seeds (Figure S1). For racemic MeCLA **10** and CL
 306 **9**, the SL biosynthetic precursors possessing the D-ring
 307 but no C ring and A ring decorated with a tertiary hydroxyl
 308 group, germination stimulation activities were drastically
 309 reduced in comparison with **14** and (±)-GR24. A small
 310 difference was observed between *P. ramosa* 1 and *P.*
 311 *ramosa* 2a for MeCLA **10** (r_{EC50} = 0.47), the putative bio-
 312 synthetic precursor of cannalactone **14**⁴⁴ (Figure 3B). The
 313 specificity of biological response would appear from the
 314 compounds downstream of MeCLA in the biosynthetic
 315 pathway. Isothiocyanates (ITCs) as glucosinolate-
 316 breakdown products are germination stimulants of *P.*
 317 *ramosa* seeds secreted in the soil by host plants as Brassi-
 318 caceae^{31,40,58}. As for (±)-MeCLA **10**, a small difference of
 319 germination was observed between *P. ramosa* 1 and *P.*
 320 *ramosa* 2a ($0.1 < r_{EC50} < 1.1$ for 2-phenylethyl isothiocya-
 321 nate)^{39,45}.

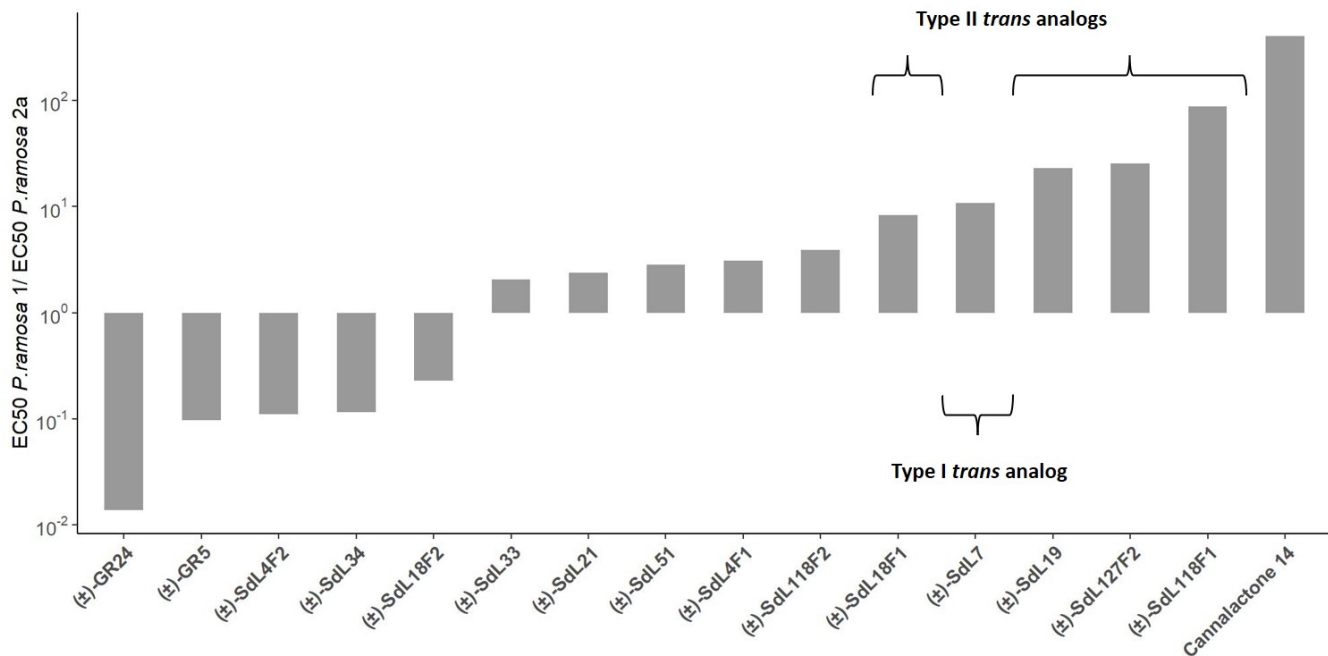


322 **Chart 3. Cannalactone analogs synthesized for this**
 323 **study.**
 324



326

327



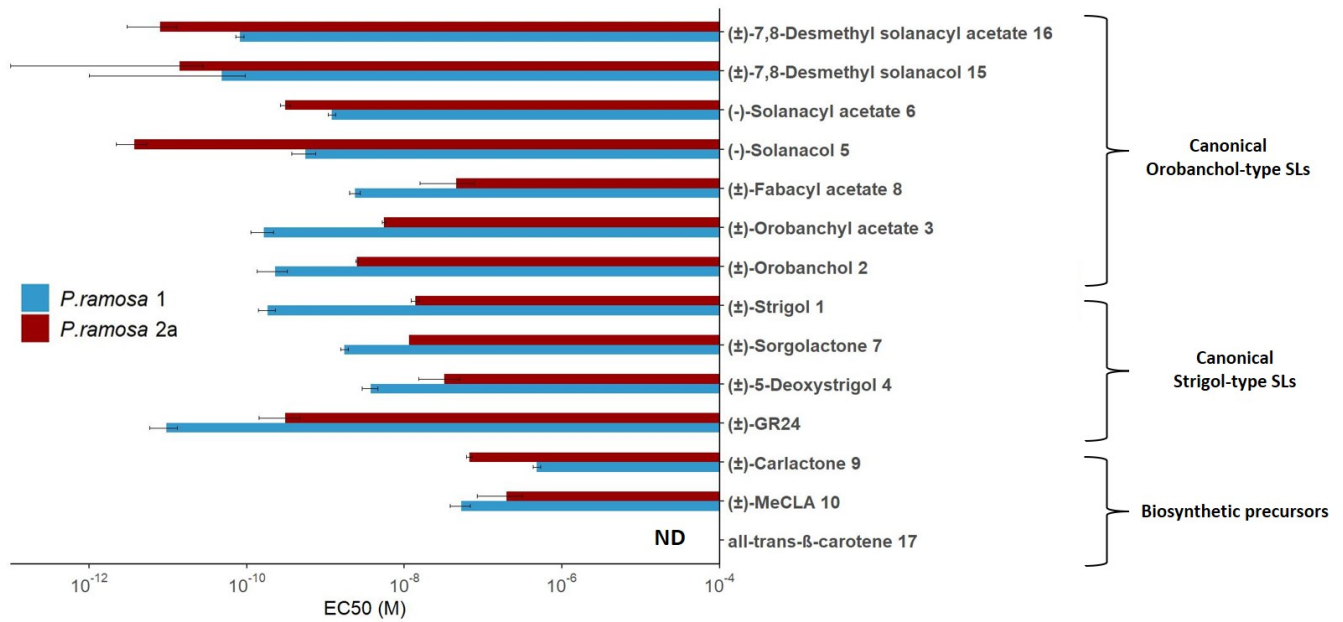
328

329 Figure 2. Bioactivity on *Phelipanche ramosa* 1 versus *Phelipanche ramosa* 2a seed germination of SdL analogs (see Chart 3). (A)
 330 EC₅₀ (half maximal effective concentration) (mol L⁻¹) of SdL analogs, (±)-GR5, natural cannalactone **14** and (±)-GR24 toward *P.*
 331 *ramosa* 1 and *P. ramosa* 2a. EC₅₀ are presented ± SE, (6 ≤ n ≤ 12). (B) $_{EC50} [EC_{50} (P. ramosa 1) / EC_{50} (P. ramosa 2a)]$ for each chemi-
 332 cal.

333

334

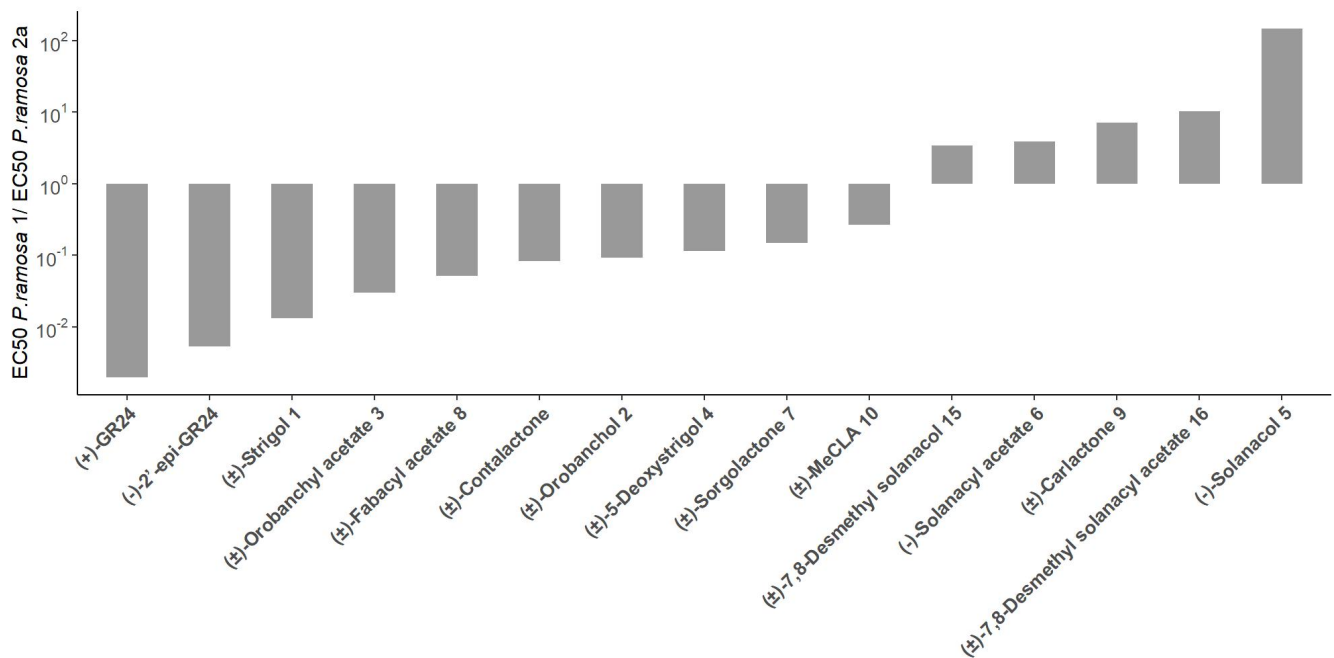
A



336

337

B



338

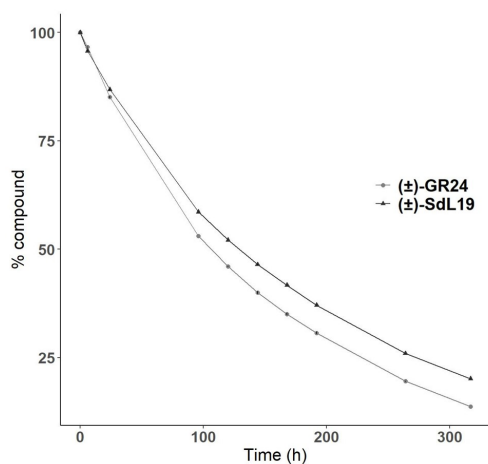
339 Figure 3. Bioactivity on *Phelipanche ramosa* 1 versus *Phelipanche ramosa* 2a seed germination of canonical SLs, SL biosynthetic
 340 precursors in comparison with (+)-GR24⁴⁵ and (-)-2'-epi-GR24⁴⁵. (A) EC₅₀ (half maximal effective concentration) (mol L⁻¹) of
 341 canonical SLs and (±)-GR24 toward *P. ramosa* 1 and *P. ramosa* 2a. EC₅₀ are presented ± SE, (6 ≤ n ≤ 12). (B) r_{EC50} = EC₅₀ (*P. ramosa* 1)/
 342 EC₅₀ (*P. ramosa* 2a) for each SL and (±)-contalactone⁴⁵. ND = not determined.

343

344 Comparing the germination stimulation activities of (±)-
 345 GR5 to that of (±)-GR24, loss of cycles A and B led to bio-
 346 activity reductions but also dampened the difference be-
 347 tween *P. ramosa* 1 and *P. ramosa* 2a (r_{EC50} ((±)-GR5) =
 348 0.10) (Figure 2B). All (±)-SdL analogs are bioactive but
 349 less than (±)-GR24 for *P. ramosa* 1. (±)-SdL118F1 and (±)-

350 SdL127F2 proved to be more bioactive toward *P. ramosa*
 351 2a while all the other SdLs were less bioactive than can-
 352 talactone even if they have high activity for this popula-
 353 tion. SdL analogs possess EC₅₀ values varying between
 354 5.6×10⁻¹⁰-4.8×10⁻⁸ M for *P. ramosa* 1, and 6.4×10⁻¹²-
 355 2.1×10⁻⁷ M for *P. ramosa* 2a. Removal of AB rings and

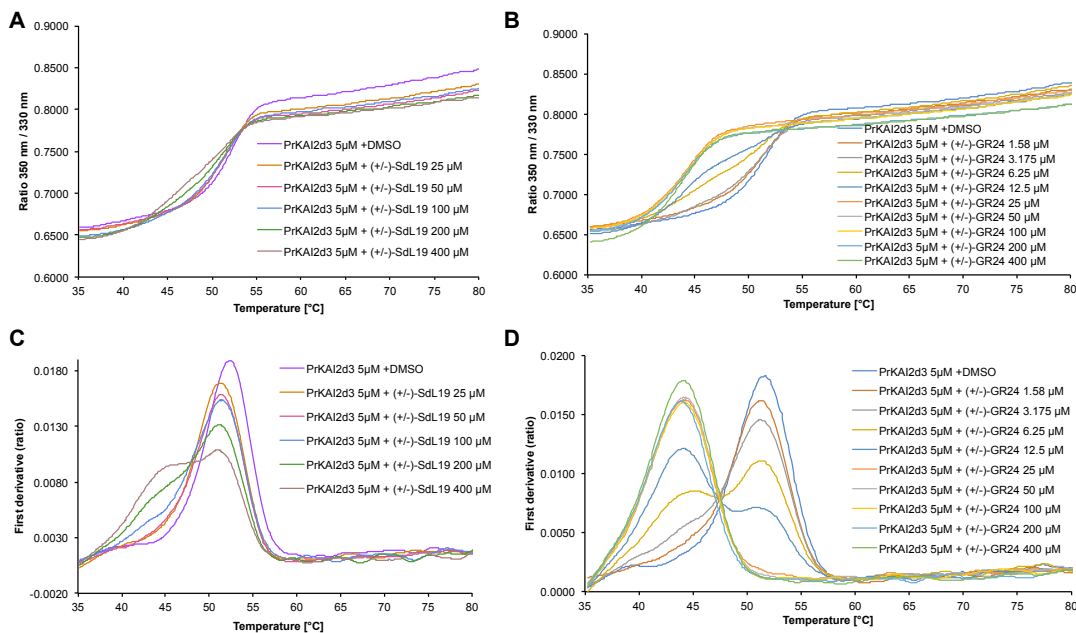
356 replacement by an unsaturated acyclic carbon chain at C-
 357 3a position induced a loss of bioactivity toward *P. ramosa*
 358 1 for all SdL analogs compared to (±)-GR24. Moreover, no
 359 significant difference was observed between “cis”
 360 (2'R*,4R*) and “trans” (2'R*,4S*) SdL analogs toward *P.*
 361 *ramosa* 1. On the other hand, on *P. ramosa* 2a seeds, SdL
 362 analogs with an acyclic unsaturated carbon chain have a
 363 bioactivity similar to (±)-GR24. For the genetic group 2a, it
 364 was also interesting to find that the (±)-trans-SdL analogs
 365 were more active than the (±)-cis-SdL analogs. It was
 366 therefore possible to classify SdL analog bioactivity using
 367 the r_{EC50} diagram (Figure 2B). The most active and selective
 368 molecules toward *P. ramosa* 2a are thus (±)-SdL118F1
 369 ($EC_{50} = 5.6 \times 10^{-10}$ M, $r_{EC50} = 87.5$), (±)-SdL19 ($EC_{50} =$
 370 1.5×10^{-10} M, $r_{EC50} = 18.7$) and (±)-SdL7 ($EC_{50} = 2.4 \times 10^{-10}$
 371 M, $r_{EC50} = 10.8$). The analog (±)-SdL19 showed a similar
 372 selectivity for the germination of *P. ramosa* 2a versus *P.*
 373 *ramosa* 1 as cannalactone **14**, and a similar bioactivity
 374 toward *P. ramosa* 2a ($EC_{50} 1.5 \times 10^{-10}$ M versus 1.0×10^{-10} M)
 375 (Figure 2A). Subsequently, due to the ease of preparation
 376 of the compound (±)-SdL19 and its specificity, we focused
 377 on this compound in the rest of this study.



378
 379 Figure 4. Stability of (±)-SdL19. Chemical hydrolysis of (±)-
 380 SdL19 and (±)-GR24 in ethanol/PBS at pH 6.8. Data are
 381 means \pm SE (n = 3).
 424

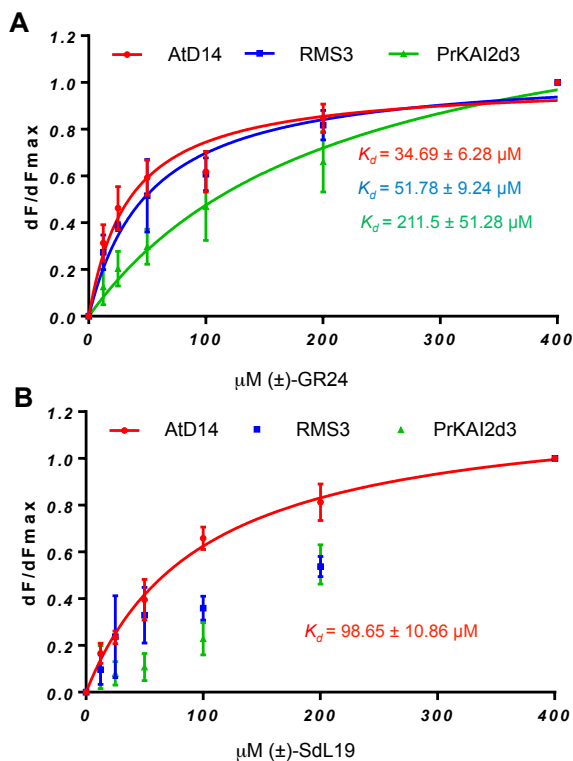
382 SLs and mimics are sensitive to hydrolysis giving for (±)-
 383 GR24 poorly active or inactive 5-hydroxy-3-methylbutenolide
 384 (D-OH)⁵¹ and inactive ABC=CHOH tricycle⁵⁹. Their sensi-
 385 tivity to hydrolysis has been tested routinely in aqueous
 386 solutions and compared to that of (±)-GR24^{23,60}, even
 387 though the assay was not performed at biologically active
 388 concentrations. Therefore, the chemical hydrolysis of (±)-
 389 SdL19 in comparison with (±)-GR24 was evaluated in a
 390 mixture of ethanol/water at pH 6.8, as previously reported
 391 for other SL analogs and mimics^{23,60}. Under these condi-
 392 tions, a slightly higher stability of (±)-SdL19 was rec-
 393 orded in comparison with (±)-GR24 ((±)-SdL19 $t_{1/2} \approx 120$
 394 h, (±)-GR24 $t_{1/2} \approx 100$ h) (Figure 4).

(±)-SdL19 cannalactone analog weakly interacts with the SL receptor PrKAI2d3. We have recently character-
 395 ized the PrKAI2d3 protein as a SL receptor from *P. ramosa*
 396 1 among five PrKAI2 candidates, and we have demon-
 397 strated its high interaction with (±)-GR24⁵¹. We tested the
 398 interaction between (±)-SdL19 and PrKAI2d3 using nano
 399 differential scanning fluorimetry (nanoDSF). NanoDSF
 400 allows to evaluate the interaction between a receptor
 401 protein and a ligand by monitoring the melting tempera-
 402 ture of the receptor protein. In nanoDSF, changes in the
 403 protein fluorescence (ratio 350 nm/330 nm) are recorded
 404 and do not require a dye. This technique can highlight
 405 interactions that induce minor conformational changes.
 406 Compared to (±)-GR24, incubation with (±)-SdL19 at low
 407 concentrations did not affect the melting temperature of
 408 PrKAI2d3. However, the use of high concentrations of (±)-
 409 SdL19 lowered the inflection point of the melting curve
 410 indicating the binding of the ligand to the protein (Figure
 411 5). We studied also the binding affinity of (±)-SdL19 to-
 412 wards PrKAI2d3 by intrinsic fluorescence but no K_a value
 413 was measurable in comparison with (±)-GR24 (Figure 6).
 414 The lower affinity of (±)-SdL19 for PrKAI2d3 in compar-
 415 ison with (±)-GR24 confirmed the nanoDSF data. These
 416 results are in accordance with the lower bioactivity of (±)-
 417 SdL19 on seeds of *P. ramosa* 1 in comparison with (±)-
 418 GR24. The characterization of SL receptor(s) from *P. ra-*
 419 *mosa* 2a is awaiting and would be appreciable to discuss
 420 the SAR results presented here in the light of ligand-
 421 protein interactions.
 422
 423



425

426 Figure 5. Biochemical analysis of the interaction between the PrKAI2d3 with (±)-GR24 and (±)-SdL19 by nanoDSF. (A, B) Thermo-
 427 stability of PrKAI2d3 at 5 μM in the absence of ligand or in the presence of various ligand concentrations. Panels (A, B) show the
 428 changes in fluorescence (ratio F_{350nm}/F_{330nm}) with temperature for (±)-SdL19 and (±)-GR24, respectively. The panels (C, D) show
 429 the first derivatives for the F_{350nm}/F_{330nm} curve against the temperature gradient from which the apparent melting temperatures
 430 (T_m) were determined for (±)-SdL19 and (±)-GR24, respectively. The experiment was carried out twice.



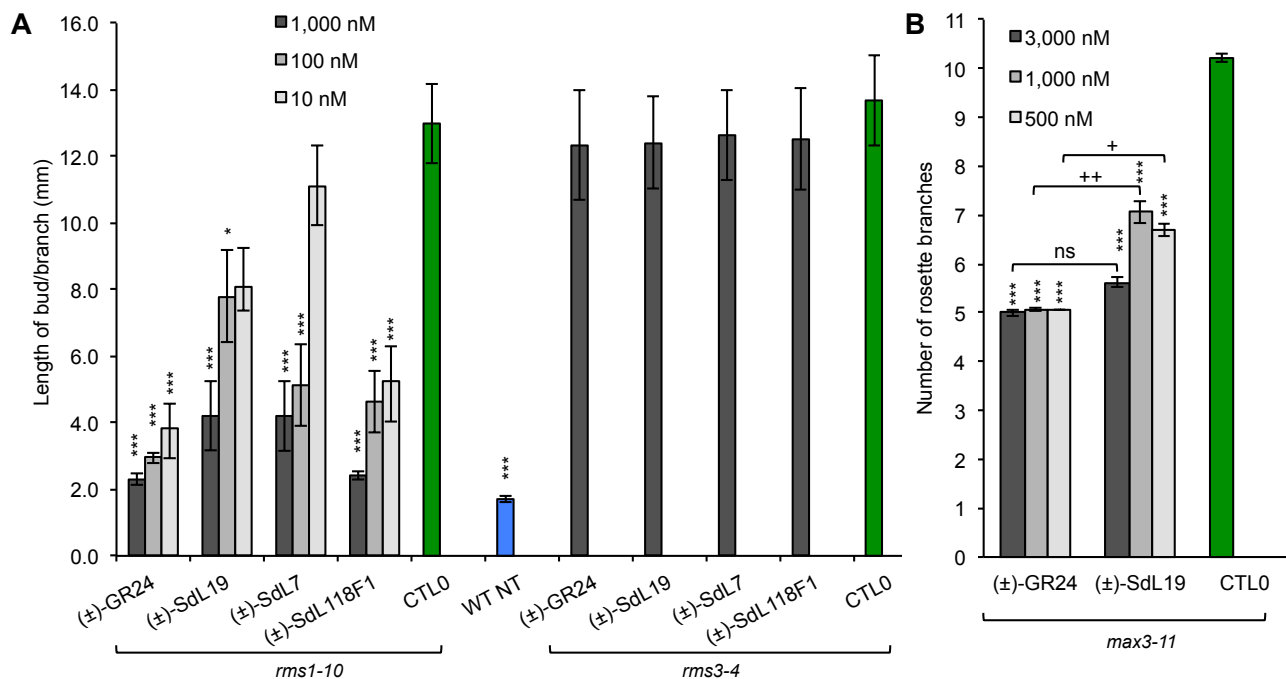
431

432 Figure 6. Biochemical analysis of the interaction between the PrKAI2d3, RMS3 and AtD14 proteins with (±)-GR24 (A) and
 433 (±)-SdL19 (B) by intrinsic tryptophan fluorescence. Plots of fluorescence intensity versus (±)-SdL19 or (±)-GR24 concen-
 434 tations were used to determine the apparent K_d values. The plots represent the mean of two replicates and the experi-
 435 ments were repeated at least three times.

467

436 trations were used to determine the apparent K_d values. The
 437 plots represent the mean of two replicates and the experi-
 438 ments were repeated at least three times.

439 **Cannalactone analogs efficiently inhibit bud out-**
 440 **growth in pea and *Arabidopsis*, and interact with SL**
 441 **receptor D14 proteins.** The biological activities of (±)-
 442 SdL analogs as plant hormones were evaluated using a
 443 pea branching assay with the highly branched SL-deficient
 444 *rms1-10* mutant⁶¹. All (±)-SdL analogs showed activity at a
 445 concentration of 1 μM but were found to be notably less
 446 active than (±)-GR24, since they were not significantly
 447 bioactive at 10 nM or below (Figure 7, Table S2). This
 448 confirms the low specificity of SL reception in pea for
 449 which a wide range of SLs, analogs and mimics are bioac-
 450 tive^{23,60}. Moreover, (±)-SdL analogs were inactive on the
 451 branching of the pea *rms3-4* perception mutant (Figure
 452 7A), Table S3). These results suggest that (±)-SdL analogs,
 453 as (±)-GR24, are bioactive SL analogs and inhibit bud
 454 outgrowth via the RMS3 receptor, an ortholog of D14 in
 455 pea, and not because of toxicity. To investigate potential
 456 species differences, we examined the effect of (±)-SdL19
 457 on *Arabidopsis* shoot branching. We applied (±)-SdL19
 458 and (±)-GR24 to the hydroponically grown *max3-11*
 459 plants. *max3-11* is a SL-deficient mutant⁶². Treatment with
 460 all concentrations of (±)-SdL19 inhibited outgrowth of
 461 axillary buds in *max3-11*. However, a significant difference
 462 was observed with (±)-GR24 for low concentrations test-
 463 ed (< 3000 nM) (Figure 7B). These results indicated that
 464 (±)-SdL19 is less active than (±)-GR24 in *Arabidopsis* for
 465 shoot branching inhibition when applied to the roots in
 466 hydroponic culture.



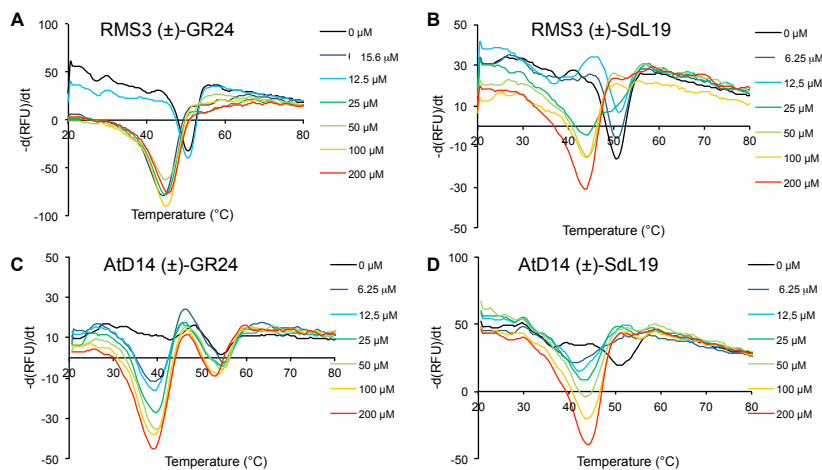
468

469 Figure 7. Bioactivity in pea and *Arabidopsis*. Bioactivity in pea of (±)-SdL7, (±)-SdL19 and (±)-SdL118F1 versus (±)-GR24 (*rms1*,
470 *rms3*) (A). Length of the axillary buds of *rms1-10* and *rms3-5* pea plants, 8 d after direct application of the various analogs; CTL0 =
471 DMSO treatment ; WT Tèrese plants were used as controls without treatment. Data are means \pm SE (≥ 20 plants) *** $P < 0.001$, * $P <$
472 0.5, Kruskal-Wallis rank sum test, compared to CTL0 value. See also supplementary data in the Supporting Information. Bioactivity
473 in *Arabidopsis* of probes versus (±)-GR24 (*max3-11*). Bioactivity in *Arabidopsis* of (±)-SdL19 versus (±)-GR24 (B). Number of rosette
474 branches of mutant plants *max3-11* grown in long-day conditions. These data were obtained from means \pm SE ($n = 16$ plants). *** P
475 < 0.001 indicate significant differences with the control treatment (0 nM) (CTL0) (Shapiro-Wilkinson normality test). + $P < 0.05$, ++
476 $P < 0.01$ indicate significant differences with (±)-GR24 treatment (Shapiro-Wilkinson normality test). ns = not significant. CTL0 =
477 control

478 In order to validate that (±)-SdL analogs are perceived by
479 the pea SL receptor RMS3, we performed differential
480 scanning fluorimetry (DSF) and revealed a shift in RMS3
481 melting temperature in the presence of (±)-SdL19, corre-
482 sponding to a protein destabilization as for the other SL
483 bioactive analogs⁴ (Figure 8A-B). We showed that the
484 destabilization of RMS3 by (±)-SdL19 was recorded at
485 higher ligand concentrations in comparison with (±)-
486 GR24 suggesting lower affinity. For AtD14, an ortholog of
487 D14 in *Arabidopsis*, DSF recordings revealed an increased
488 sensitivity for (±)-SdL19, inversely for (±)-GR24 as pre-
489 viously reported for cannalactone **14**⁴⁴ and in contrast to
490 RMS3 (Figure 8C-D). These results are in accordance with

491 the fact that in pea, the main SLs detected are canonical
492 SLs⁶³, while in *Arabidopsis*, no canonical SL has been de-
493 tected but only non-canonical SLs or their biosynthetic
494 precursors such as methyl carlactonoate ((+)-MeCLA **10**)
495 and HO-MeCLAs^{12,13}. Then, we estimated the binding affini-
496 ty of (±)-SdL19 towards RMS3 and AtD14 by intrinsic
497 fluorescence and found a measurable K_d value ($98.65 \pm$
498 $10.86 \mu\text{M}$) only for AtD14 (Figure 6B). The lower affinity
499 of (±)-SdL19 for RMS3 in comparison with AtD14 high-
500 lights differences between biochemical and *in planta* re-
501 sults where in both *Arabidopsis* and pea, (±)-SdL19 is less
502 bioactive than (±)-GR24 for bud outgrowth inhibition.

503



504

505 Figure 8. Biochemical analysis of the interaction RMS3/PsD14, AtD14 proteins with (±)-GR24 and (±)-SdL19. The melting temperature curves of RMS3 (A, B) and AtD14 (C, D) proteins with varying indicated concentrations of (±)-GR24 and (±)-SdL19, as assessed by DSF, are shown. Each line represents the average protein melt curve for three technical replicates and the experiment was carried out three times.

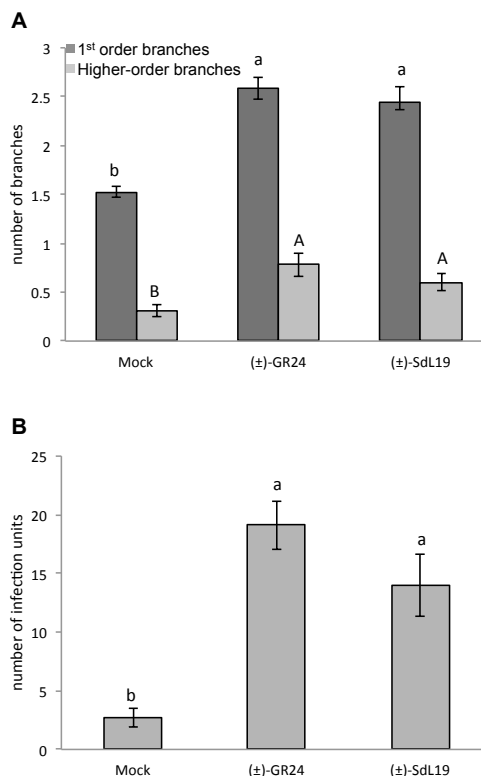
509 **(±)-SdL19 cannalactone analog promotes hyphal branching in the AM fungus *Rhizophagus irregularis*.**

510 The SL analogs produced in the present study can also help to address SAR in AM symbiosis. SLs are known to induce a number of developmental, cellular and metabolic responses in AM fungi³⁴⁻³⁶. In particular, the stimulation of hyphal branching is commonly used in bioassays to detect the bioactivity of SLs on these fungi. Using this approach, a number of SLs and related compounds have been tested for their activity on the AM fungus *Gigaspora margarita*. Taken together, these studies highlighted the complexity of structural requirements in the ABC moiety. GR5 was shown to be inactive, and early studies proposed that a minimal structure would contain the C-D moiety fused to at least one ring system^{35,64}. This proposal is consistent with the recent discovery of bioactive bryosymbiol **13** carrying A, C and D rings²². However, results obtained with CL derivatives later indicated that some compounds without a C ring could retain activity²⁶. Combined with reports on natural non-canonical SLs bearing variations on the A or C rings⁶, these studies indicate that requirements for bioactivity on AM fungi can be fulfilled in several divergent ways.

532 In the present study, we first used an *in vitro* assay which allows a quantification of hyphal branching⁶⁵ in the AM fungus *Rhizophagus irregularis*. As shown in Figure 9A, (±)-SdL19 stimulated hyphal branching (*i.e.* the formation of first-order and higher-order branches) in a similar fashion to (±)-GR24. This indicates that a C-D moiety combined with an acyclic carbon chain is sufficient for bioactivity on this AM fungus.

540 The hyphal branching response triggered by SL analogs is commonly used as a proxy measure for the stimulation of the fungal symbiont, but this response does not always reflect the ability of these compounds to facilitate the initiation of symbiosis⁶⁵. To further document the ability of (±)-SdL19 to stimulate *R. irregularis* in a true symbiotic context, we used an additional test. This assay involves *Medicago truncatula* plants mutated in the SL biosynthesis gene *CCD8*. These mutants are strongly affected in

549 their ability to initiate symbiosis with *R. irregularis*, and this phenotype can be rescued by exogenous application of SL analogs⁶⁵. Like other bioassays involving SL biosynthesis plant mutants and designed to investigate the hormonal activities of SL analogs, this test records the ability of these analogs to “replace” natural SLs in a physiological context. Using this assay, we have previously shown the bioactivity of cannalactone **14** in AM symbiosis⁴⁴, indicating that the B ring is dispensable. In the present study, we found that (±)-SdL19 exhibited an activity similar to (±)-GR24 (Figure 9B). This extends our previous observations by showing that symbiotic activity can be conserved when both A and B rings are absent and replaced by an unsaturated acyclic carbon chain.



563

564 Figure 9. Activity of (±)-SdL19 on the development of *R.*
565 *irregularis* and its symbiotic ability. (A) *R. irregularis* was
566 grown from spores for 12 days on medium containing 10⁻⁷ M
567 (±)-GR24 or (±)-SdL19, or the solvent alone (mock), then the
568 number of branches of first order (black bars) and higher
569 order (grey bars) were measured. Bars represent the mean ±
570 SE, n = 6 to 8 plates per condition, representing an average of
571 200 spores. (B) *R. irregularis* spores were used to inoculate
572 *M. truncatula ccd8-1* SL-deficient plants. 10⁻⁷ M (±)-GR24 or
573 (±)-SdL19, or the solvent alone (mock) were supplied in the
574 nutrient solution. The ability of (±)-SdL19 to restore symbi-
575 otic ability in *R. irregularis* was assessed by examining root
576 colonization, 23 days post-inoculation. Bars represent the
577 mean number of infection units per plant ± s.e.m. n = 14 to 16
578 plants per condition. Bars topped with the same letter do not
579 differ significantly by Mann-Whitney U test (*P* > 0.05).

580 To conclude, we provide with this study comprehensive
581 SAR data in two genetic groups of *P. ramosa*, comprising
582 routes for synthesis of 14 analogs (SdL) of the non-
583 canonical SL cannalactone **14**. The SdL analogues with the
584 best specificity towards the population 2a are the com-
585 pounds with a polar part on the side carbon chain. In
586 addition to non-canonical SL cannalactone **14** recently
587 identified from hemp in our group⁴⁴, natural canonical SLs
588 (-)-solanacol **5** and (-)-solanacyl acetate **6** exuded by
589 tobacco^{41,42} and tomato⁶⁶, host plants for *P. ramosa* 2a^{38,39},
590 are reported here as remarkable selective germination
591 stimulants for *P. ramosa* 2a seeds, contrary to other SLs
592 such as orobanchol **2**, orobanchyl acetate **3** and 5-
593 deoxystrigol **4**, also detected in tobacco root exudates⁴².
594 Our data further extend common knowledge on SL ana-
595 logs that are involved in plant and AM fungi development.
596 Further studies on the interaction of those substances
597 with specific receptors in AM fungi, key players for a sus-
598 tainable agriculture, and in *P. ramosa* 2a, will help to fully
599 resolve the structure–activity relationships in these spe-
600 cies⁶⁵. Moreover, these highly active non-canonical SLs
601 (e.g., (±)-SdL19) could be useful for the study of other
602 organisms which putatively produce only non-canonical
603 SLs such as the moss *Physcomitrium patens*^{66,67,68} and *Ara-*
604 *bidopsis thaliana*¹³.

605 EXPERIMENTAL SECTION

607 **Synthesis: General experimental procedures.** All non-
608 aqueous reactions were run under an inert atmosphere
609 (argon), by using standard techniques for manipulating
610 air-sensitive compounds. All glassware was stored in the
611 oven and/or was flame-dried prior to use. Anhydrous
612 solvents were obtained by filtration through drying col-
613 umns. Analytical thin-layer chromatographies (TLC) were
614 performed on plates precoated with silica gel layers.
615 Compounds were visualized by one or more of the follow-
616 ing methods: (1) illumination with a short wavelength UV
617 lamp (i.e., λ = 254 nm), (2) spray with a 1% (w/v) KMnO₄
618 solution in H₂O. All separations were carried out under
619 flash-chromatographic conditions on silica gel (prepacked
620 column, 230 – 400 mesh) at medium pressure (20 psi)
621 with Armen fraction collector and pump. Nuclear magnet-
622 ic resonance spectra (¹H; ¹³C NMR) were recorded respec-
623 tively at [500 or 300; 175, 125 or 75] MHz on recorded on
624 Bruker Avance spectrometers at 298 K. For the ¹H spec-

625 tra, data are reported as follows: chemical shift, multiplic-
626 ity (s = singlet, d = doublet, t = triplet, q = quartet, m =
627 multiplet, b = broad, coupling constant in Hz and integra-
628 tion. The numbering for signal assignment was done ac-
629 cording to Chart 2. IR spectra are reported in reciprocal
630 centimeters (cm⁻¹). Buffers and aqueous mobile-phases
631 for UPLC were prepared using water purified with a Milli-
632 Q system. Mass spectra (MS) and high-resolution mass
633 spectra (HRMS) were determined by electrospray ioniza-
634 tion (ESI) coupled to a time-of-flight analyzer (Waters
635 LCT Premier XE, Waters, USA) or with an Ultra Perform-
636 ance Liquid Chromatography system equipped with a
637 Triple Quadrupole mass spectrometer Detector (Acquity
638 UPLC-TQD, Waters, USA).

639 All-*trans*-β-carotene **17** is commercially available. (±)-
640 GR24 was prepared according to known procedures⁶⁹ and
641 careful purification (HPLC)⁴⁵. (±)-GR5 was synthesized by
642 known procedures²¹. (±)-MeCLA was prepared by an
643 unpublished method (Lucile Andna, Laurence Miesch).
644 (±)-Carlactone was synthesized by Adrian Scaffidi⁷⁰. Natu-
645 ral cannalactone **14** was isolated as described in
646 Hamzaoui et al⁴⁴. (±)-Strigol **1**, (±)-5-deoxystrigol **4**, (±)-
647 sorgolactone **5**, (±)-orobanchol **2** are commercially avail-
648 able. Orobanchyl acetate **3** was synthesized from (±)-
649 orobanchol by acetylation with acetic anhydride in pyri-
650 dine as described in Boutet et al⁷¹. (-)-Solanacol **5** and
651 (-)-solanacyl acetate **6** are obtained as described in Boyer
652 et al²³ and (±)-7,8-desmethyl solanacol **15** and (±)-7,8-
653 desmethyl solanacyl acetate **16** as described in Chen et
654 al⁷². (±)-Fabacyl acetate **7** was kindly furnished by Koichi
655 Yoneyama. (±)-4-Vinyldihydrofuran-2(3*H*)-one **19** was
656 prepared by a known procedure⁵².

657 **(2′R*,4R*)-SdL4F1 and (2′R*,4S*)-SdL4F2.** A mixture of
658 alkene **19** (200 mg, 1.78 mmol), ethyl formate (144 μL,
659 1.96 mmol) in THF (4 mL) was placed at -78 °C. Potassi-
660 um *tert*-butoxide was added (240 mg, 2.14 mmol). The
661 mixture was stirred for 2 h at -78 °C. A solution of bro-
662 mide derivative **20**⁷³ (350 mg, 1.96 mmol) in THF (3.2
663 mL) was added. The mixture was stirred at room temper-
664 ature during 12 h. The mixture was diluted with EtOAc
665 and saturated NH₄Cl aqueous solution and then separat-
666 ed. The organic phase was washed with water and brine.
667 The combined organic layers were dried with Na₂SO₄,
668 filtered and evaporated under reduced pressure. The
669 mixture was purified by chromatography on silica gel
670 (heptane/EtOAc 80: 20 to 60: 40 during 30 min) to afford
671 pure (±)-SdL4F1 (87.5 mg, 21%) and (±)-SdL4F2 (85.7
672 mg, 20%) as a brown oils. (±)-SdL4F1: ¹H NMR (300 MHz,
673 CDCl₃) δ: 7.51 (d, *J* = 2.0 Hz, H10), 6.88 (t, *J* = 1.5 Hz, H6′),
674 6.12 (t, *J* = 1.5 Hz, H2′), 5.81-5.70 (m, H6), 5.12 (dt, *J* = 1.0,
675 6.0 Hz, H7a), 5.08 (d, *J* = 1.0 Hz, H7b), 4.41 (t, *J* = 9.0 Hz,
676 H5a), 4.07 (q, *J* = 4.5 Hz, H5b), 3.83-3.74 (m, H4), 1.97 (t, *J*
677 = 1.5 Hz, 3 H7′). ¹³C NMR (75 MHz, CDCl₃) δ: 171.5 (C5′),
678 170.4 (C2), 151.7 (C6′), 141.1 (C3′), 135.9 (C4′), 135.4
679 (C6), 116.7 (C7), 109.9 (C3), 100.7 (C2′), 71.1 (C5), 40.6
680 (C4), 10.9 (C7′). IR (cm⁻¹): 3092, 2983, 2919, 2850, 1781,
681 1752, 1683, 1344, 1207, 1184, 1083, 1026, 955, 866,
682 801 745. HRMS (ESI): Calcd for C₁₂H₁₃O₅ [M + H]⁺:
683 237.0763, found: 237.0762. (±)-SdL4F2: ¹H NMR (300
684 MHz, CDCl₃) δ: 7.48 (d, *J* = 2.0 Hz, H10), 6.88 (t, *J* = 1.5 Hz,
685 H6′), 6.12 (t, *J* = 1.5 Hz, H2′), 5.79-5.68 (m, H6), 5.10 (dt, *J*

686 = 1.0, 6.0 Hz, H7a), 5.06 (d, $J = 1.0$ Hz, H7b), 4.40 (t, $J = 9.0$
687 Hz, H5a), 4.05 (q, $J = 4.5$ Hz, H5b), 3.82-3.74 (m, H4), 1.96
688 (t, $J = 1.5$ Hz, 3 H7'). ^{13}C NMR (75 MHz, CDCl_3) δ : 171.5
689 (C5'), 170.4 (C2), 151.4 (C6'), 141.3 (C3'), 136.0 (C4'),
690 135.1 (C6), 116.9 (C7), 110.0 (C3), 100.6 (C2'), 71.0 (C5),
691 40.5 (C4), 10.9 (C7'). IR (cm^{-1}): 3089, 2917, 2850, 1775,
692 1747, 1679, 1342, 1181, 1082, 1003, 950. HRMS (ESI):
693 Calcd for $\text{C}_{12}\text{H}_{13}\text{O}_5$ [$\text{M} + \text{H}$] $^+$: 237.0768, found: 237.0762.

694 **(2'R*,4R*)-SdL7**. To a solution of (\pm)-SdL4F1 (76.5 mg,
695 0.32 mmol, 1 equiv) in CH_2Cl_2 (0.36 mL), was added meth-
696 yl acrylate (0.294 mL, 3.24 mmol, 10 equiv) and Hove-
697 yda-Grubbs II metathesis initiator (HGII) (10.9 mg, 0.016
698 mmol, 5 mol%) under argon. The mixture was stirred for
699 24 h at 50 °C in a closed flask with rodavis cap. The mixture
700 was purified by chromatography on silica gel (hep-
701 tane/EtOAc 40: 60) to afford pure (\pm)-SdL7 (54.4 mg,
702 57%, brown oil). ^1H NMR (300 MHz, CDCl_3) δ : 7.58 (d, $J =$
703 2.0 Hz, H6'), 6.87 (t, $J = 2.0$ Hz, H3'), 6.80 (dd, $J = 8.0, 15.5$
704 Hz, H6), 6.12 (t, $J = 2.0$ Hz, H2'), 5.88 (dd, $J = 1.0, 15.5$ Hz,
705 H7), 4.46 (t, $J = 8.5$ Hz, H5a), 4.13 (dd, $J = 3.5, 9.5$ Hz, H5b),
706 4.00-3.90 (m, H4), 3.73 (s, 3 H9), 1.99 (s, 3 H7'). ^{13}C NMR
707 (75 MHz, CDCl_3) δ : 170.6 (C2), 170.3 (C5'), 166.5 (C8),
708 152.7 (C6'), 144.3 (C6), 140.9 (C3'), 136.1 (C4'), 122.9
709 (C7), 108.5 (C3), 100.8 (C2'), 69.9 (C5), 52.0 (C9), 39.1
710 (C4), 10.9 (C7'). $J_{\text{C}_2\text{-H}_6}$ = 2.0 Hz. IR (cm^{-1}): 3096, 2959,
711 2919, 2850, 1782, 1756, 1721, 1683, 1437, 1348, 1280,
712 1186, 1091, 1033, 1010, 956, 867, 748. HRMS (ESI): Calcd
713 for $\text{C}_{16}\text{H}_{17}\text{NO}_7\text{Na}$ [$\text{M} + \text{CH}_3\text{CN} + \text{Na}$] $^+$: 358.0903, found:
714 358.0903.

715 **4-(3-Oxobut-1-en-1-yl)dihydrofuran-2(3H)-one (21)**.
716 To a solution of 4-vinyldihydrofuran-2(3H)-one **19** (400.4
717 mg, 3.57 mmol, 1 equiv) in CH_2Cl_2 (4 mL), was added
718 buten-3-one (2.98 mL, 35.70 mmol, 10 equiv) and HGII
719 (110.4 mg, 0.17 mmol, 5 mol%) under argon. The mixture
720 was stirred for 24 h at 50 °C in a closed flask with rodavis
721 cap. The mixture was purified by chromatography on
722 silica gel (heptane/EtOAc 70 : 30 to 50 : 50 during 30
723 min) to afford pure ketone **21** as a brown oil (375.9 mg,
724 68%). ^1H NMR (300 MHz, CDCl_3) δ : 6.66 (dd, $J = 7.5, 15.5$
725 Hz, H6), 6.17 (dd, $J = 1.0, 16.0$ Hz, H7), 4.48 (dd, $J = 7.5,$
726 11.5 Hz, H5a), 4.08 (dd, $J = 7.5, 11.5$ Hz, H5b), 3.38 (sext, J
727 = 8.0 Hz, H4), 2.74 (dd, $J = 7.5, 16.0$ Hz, H3a), 2.44 (dd, $J =$
728 7.5, 16.0 Hz, H3b), 2.25 (s, 3 H9). ^{13}C NMR (75 MHz,
729 CDCl_3) δ : 197.5 (C2), 175.4 (C8), 142.9 (C6) 132.5 (C7),
730 71.4 (C5), 38.6 (C4), 34.0 (C3), 27.8 (C9). IR (cm^{-1}): 3000,
731 2913, 1771, 1672, 1629, 1360, 1257, 1162, 1015, 979,
732 890, 838. UPLC-TQD (MS): m/z 155.2 [$\text{M} + \text{H}$] $^+$, 100%.

733 **(E)-4-(3-Hydroxy-3-methylbut-1-en-1-yl)dihydrofuran-2(3H)-one (21a)**. THF (20 mL) was
734 added to anhydrous CeCl_3 (800.0 mg, 3.24 mmol, 1.4
735 equiv), dried by heating at 140 °C/30 rpm for 2 h, 0 °C.
736 The mixture was stirred overnight under argon at room
737 temperature. At this temperature, a solution of ketone **21**
738 (357.3 mg, 2.32 mmol) in THF (11.5 mL) was added and
739 stirred for 1 h. Then it was cooled to -70 °C and a solution
740 of methylmagnesium chloride in THF (1.1 mL (3 M), 3.24
741 mmol, 1.4 equiv) was added by syringe. The reaction
742 mixture was stirred until TLC indicated disappearance of
743 starting material. The reaction was quenched with an
744 aqueous 10% acetic acid solution (20 mL) and extracted
745 with EtOAc (3 \times 10 mL). The organic layer was washed
746

747 with water (2 \times 10 mL) and brine (10 mL). The combined
748 organic layers were dried with Na_2SO_4 , filtered and evap-
749 orated under reduced pressure to afford crude product
750 **22a** as a brown oil (381.8 mg, 96%) used in the next step
751 without further purification but which can be also puri-
752 fied by chromatography on silica gel (heptane/EtOAc 40:
753 60) to afford pure alcohol **22a**. ^1H NMR (300 MHz, CDCl_3)
754 δ : 5.75 (dd, $J = 1.0, 15.5$ Hz, H6), 5.59 (dd, $J = 8.0, 15.5$ Hz,
755 H7), 4.41 (dd, $J = 8.0, 10.0$ Hz, H5a), 3.97 (t, $J = 8.5$ Hz,
756 H5b), 3.19 (sext, $J = 8.5, 17.5$ Hz, H3a), 2.65 (dd, $J = 8.5, 17.5$ Hz,
757 H3b), 2.34 (dd, $J = 9.5, 17.5$ Hz, H3b), 1.30 (s, 3 H9 and 3
758 H10). ^{13}C NMR (75 MHz, CDCl_3) δ : 176.7 (C2), 141.3 (C7),
759 124.5 (C6), 72.8 (C8), 70.7 (C5), 38.8 (C4), 34.8 (C3), 30.0
760 (C9 or C10), 20.4 (C9 or C10). IR (cm^{-1}): 3446, 2973, 2921,
761 1774, 1677, 1464, 1420, 1374, 1170, 1043, 1015, 975,
762 908, 839, 796, 690. UPLC-TQD (MS): m/z 93.1 (100%),
763 153.2 [$\text{M} - \text{H}_2\text{O}$] $^+$, 90%.

764 **Preparation of cyclopropylmagnesium bromide**⁷⁴. To
765 a stirred suspension of magnesium turnings (300 mg,
766 12.30 mmol) in dry THF (2.0 mL) under argon was added
767 commercially available cyclopropyl bromide (0.800 mL,
768 9.99 mmol) in dry THF (12.2 mL) dropwise at room tem-
769 perature over 30 min. During this operation, the reaction
770 continued refluxing without heating. After the addition of
771 the halide was completed, the mixture was stirred at
772 room temperature for 5 h. The titration was performed as
773 described in Sugano et al⁷⁴.

774 **(E)-4-(3-cyclopropyl-3-hydroxybut-1-en-1-yl)dihydrofuran-2(3H)-one (22b)**. Ground CeCl_3 (455.5
775 mg, 1.80 mmol, 1.4 equiv) was dried by heating at
776 140 °C/30 rpm for 2 h. Dry THF (11 mL) was added at
777 0 °C. The mixture was stirred overnight under argon at
778 room temperature. At this temperature, a solution of
779 ketone **21** (204.8 mg, 1.32 mmol) in 4 mL of dry THF was
780 added and left to stir for 1 h. Then it was cooled to -70 °C
781 and cyclopropylmagnesium bromide (5.6 mL, 0.32 M, 1.80
782 mmol, 1.4 equiv) was added by syringe. The reaction
783 mixture was left to stir until TLC indicated that no start-
784 ing material remained. The reaction was quenched with
785 an aqueous 10% acetic acid solution (10 mL) and extract-
786 ed with EtOAc (3 \times 10 mL). The organic layer was washed
787 with water (2 \times 10 mL) and brine (10 mL). The combined
788 organic layers were dried (Na_2SO_4). Solvent was removed
789 to afford crude product **22b** (266.4 mg, quantitative) used
790 in the next step without further purification but which
791 can be also purified by chromatography on silica gel (hep-
792 tane/EtOAc 40: 60) to afford pure alcohol **22b**. ^1H NMR
793 (300 MHz, CDCl_3) δ : 5.64 (s, H7), 5.62 (s, H6), 4.40 (t, J
794 = 8.5 Hz, H5a), 3.97 (t, $J = 8.0$ Hz, H5b), 3.19 (sext, $J = 8.0$
795 Hz, H4), 2.64 (dd, $J = 8.5, 17.5$ Hz, H3a), 2.33 (dd, $J = 9.0,$
796 17.5 Hz, H3b), 1.23 (s, 3H10), 1.01-0.92 (m, H9), 0.40 (d, J
797 = 8.0 Hz, 2H11 or 2H12), 0.28 (d, $J = 5.5$ Hz, 2H11 or
798 2H12). ^{13}C NMR (75 MHz, CDCl_3) δ : 176.6 (C2), 139.0 (C7),
799 125.8 (C6), 72.8 (C5), 71.6 (C8), 38.9 (C4), 34.9 (C3), 27.5
800 (C10), 21.6 (C9), 1.1 (C11 or C12), 0.97 (C11 or C12). IR
801 (cm^{-1}): 3446, 2921, 2851, 1777, 1462, 1423, 1373, 1171,
802 1045, 1016, 977, 737. HRMS (ESI): Calcd for $\text{C}_{11}\text{H}_{17}\text{O}_3$ [$\text{M} +$
803 H] $^+$: 197.1178, found: 197.1180.

805 **(E)-4-(3-Methyl-3-((trimethylsilyl)oxy)but-1-en-1-yl)dihydrofuran-2(3H)-one (23a)**. A mixture of alcohol
806 **22a** (137 mg, 0.80 mmol) and TMS-imidazole (7.4 mL,
807

808 50.39 mmol, 62.6 equiv) were stirred at 50 °C under argon for 1 h. The mixture was stirred at room temperature for 1 h and diluted with heptane (20 mL). The organic layer was washed with brine (2 × 10 mL), dried with Na₂SO₄, filtered and evaporated under reduced pressure to afford pure product **23a** (136.2 mg, 70%). ¹H NMR (300 MHz, CDCl₃) δ: 5.66 (dd, *J* = 1.0, 15.5 Hz, H6), 5.46 (dd, *J* = 8.0, 15.5 Hz, H7), 4.38 (dd, *J* = 8.0, 9.0 Hz, H5a), 3.95 (t, *J* = 9.0 Hz, H5b), 3.16 (sext, *J* = 8.5, H4), 2.62 (dd, *J* = 8.0, 17.5 Hz, H3a), 2.31 (dd, *J* = 9.5, 17.5 Hz, H3b), 1.26 (s, 3 H9 and 3 H10), 0.07 (s, 9 H TMS). ¹³C NMR (75 MHz, CDCl₃) δ: 176.7 (C2), 142.2 (C7), 123.8 (C6), 73.2 (C8), 72.8 (C5), 38.9 (C4), 34.7 (C3), 30.5 (C9 and C10), 2.7 (C TMS). IR (cm⁻¹): 2966, 2918, 1783, 1377, 1362, 1250, 1165, 1038, 1019, 972, 839, 755. UPLC-TQD (MS): *m/z* 153.3 ([M - OTMS]⁺, 100%), 93.2 (90%).

824 **(E)-4-(3-cyclopropyl-3-((trimethylsilyl)oxy)but-1-en-1-yl)dihydrofuran-2(3H)-one (23b)**. A mixture of alcohol **22b** (240.7 mg, 1.23 mmol) and TMS-imidazole (7.22 mL, 49.20 mmol, 40 equiv) were stirred at 50 °C under argon during 1 h. The mixture was stirred at room temperature during 1 h and diluted with 20 mL of heptane. The organic layer was washed with brine (2 × 10 mL), dried over Na₂SO₄ and evaporated. The mixture was purified by chromatography on silica gel (4 g, heptane/EtOAc 80:20) to afford pure product **23b** (222.4 mg, 67%). ¹H NMR (300 MHz, CDCl₃) δ: 5.62 (d, *J* = 15.5 Hz, H6), 5.52 (dd, *J* = 7.5, 15.5, H7), 4.40 (dd, *J* = 8.0, 9.0, H5a), 3.97 (t, *J* = 8.5, H5b), 3.18 (sext, *J* = 8.0, H4), 2.64 (dd, *J* = 8.5, 17.5 Hz, H3a), 2.33 (dd, *J* = 9.5, 17.5 Hz, H3b), 1.25 (s, 3 H10), 0.88-0.78 (m, H9), 0.35-0.25 (m, 2 H11 and 2 H12), 0.06 (s, 9 HTMS). ¹³C NMR (75 MHz, CDCl₃) δ: 176.7 (C2), 140.4 (C7), 125.0 (C6), 74.0 (C8), 72.8 (C5), 38.9 (C4), 34.8 (C3), 27.3 (C10), 22.2 (C9), 2.7 (C11 or C12), 1.3 (C11 or C12). IR (cm⁻¹): 3007, 2958, 2894, 1785, 1702, 1420, 1372, 1250, 1209, 1165, 1095, 1065, 1018, 975, 887, 839, 754, 685. HRMS (ESI): Calcd for C₁₄H₂₄O₃Si [M - OTMS]⁺: 179.1072, found: 179.1070.

846 **(2'R*,4R*)-SdL18F1 and (2'R*,4S*)-SdL18F2**. A mixture of compound **23a** (363.4 mg, 1.5 mmol), ethyl formate (0.12 mL, 1.50 mmol, 1.0 equiv) in THF (3 mL) was placed at -78 °C. Potassium *tert*-butoxide was added (190.7 mg, 1.70 mmol, 1.13 equiv). The mixture was stirred for 2 h. A solution of bromide derivative **20** (286.7 mg, 1.60 mmol, 1.1 equiv) in THF (3 mL) was added. The mixture was stirred at room temperature for 12 h. The mixture was diluted with EtOAc and saturated NH₄Cl aqueous solution. The organic phase was washed with water and brine. The combined organic layers were dried with Na₂SO₄, filtered and evaporated under reduced pressure. The mixture was purified by chromatography on silica gel (heptane/EtOAc 80: 20 to 70: 30 in 20 min) to afford products (±)-SdL18F1 and (±)-SdL18F2 as brown oils ((±)-SdL18F1: 100.7 mg (18%) and (±)-SdL18F2: 86.0 mg (16%), total: 34%). (±)-SdL18F1: ¹H NMR (300 MHz, CDCl₃) δ: 7.50 (d, *J* = 2.5 Hz, H6'), 6.82 (t, *J* = 1.5 Hz, H3'), 6.08 (t, *J* = 1.5 Hz, H2'), 5.64 (d, *J* = 15.5 Hz, H7), 5.48 (dd, *J* = 7.5, 15.5 Hz, H6), 4.43 (t, *J* = 9.0 Hz, H5a), 4.06 (q, *J* = 4.0 Hz, H5b), 3.82-3.74 (m, H4), 1.99 (t, *J* = 1.5 Hz, 3 H7'), 1.27 (s, 3 H9 and 3 H10), 0.09 (s, 9 HTMS). ¹³C NMR (75 MHz, CDCl₃) δ: 171.6 (C2), 170.3 (C5'), 151.6 (C6'), 141.4 (C3'), 141.0 (C7),

869 136.0 (C4'), 123.6 (C6), 110.6 (C3), 100.7 (C2'), 73.4 (C8), 71.5 (C5), 39.5 (C4), 30.7 (C9 or C10), 30.6 (C9 or C10), 10.9 (C7'), 2.8 (3C TMS). IR (cm⁻¹): 2967, 2925, 1785, 1754, 1683, 1380, 1344, 1250, 1183, 1082, 1031, 956, 840, 752. HRMS (ESI): Calcd for C₁₅H₁₇O₅Na [M + Na - OTMS]⁺: 317.1001, found: 317.1004. (±)-SdL18F2: ¹H NMR (300 MHz, CDCl₃) δ: 7.50 (d, *J* = 2.5 Hz, H6'), 6.88 (t, *J* = 1.5 Hz, H3'), 6.11 (t, *J* = 1.5 Hz, H2'), 5.63 (d, *J* = 15.5 Hz, H7), 5.45 (dd, *J* = 7.5, 15.5 Hz, H6), 4.42 (t, *J* = 9.0 Hz, H5a), 4.03 (q, *J* = 4.5 Hz, H5b), 3.81-3.72 (m, H4), 1.96 (t, *J* = 1.5 Hz, 3 H7'), 1.22 (s, 3 H9 or 3 H10), 1.20 (s, 3 H9 or 3 H10), 0.05 (s, 9 HTMS). ¹³C NMR (75 MHz, CDCl₃) δ: 171.7 (C2), 170.3 (C5'), 151.6 (C6'), 141.5 (C3'), 141.1 (C7), 136.0 (C4'), 123.3 (C6), 110.5 (C3), 100.6 (C2'), 73.4 (C8), 71.5 (C5), 39.5 (C4), 30.7 (C9 or C10), 30.4 (C9 or C10) 10.8 (C7'), 2.7 (3C TMS). IR (cm⁻¹): 2967, 2925, 1786, 1755, 1683, 1380, 1344, 1264, 1183, 1084, 1032, 956, 840, 735. HRMS (ESI): Calcd for C₁₅H₁₇O₅Na [M + Na - OTMS]⁺: 317.1001, found: 317.0998.

888 **(2'R*,4R*)-SdL19**. To a solution of scandium trifluoromethanesulfonate (0.66 mg, 1.3 μmol) in CH₃CN (1.5 mL) was added silyl derivative (±)-SdL18F1 (98 mg, 0.27 mmol) in CH₃CN (1.0 mL) and water (2.5 μL, 0.14 μmol) at room temperature. The resulting mixture was stirred for 1 h at room temperature and quenched with a phosphate buffer (pH 7). The organic materials were extracted with dichloromethane (3 × 10 mL), the combined extracts were washed with brine, dried with Na₂SO₄, filtered and evaporated under reduced pressure to afford pure (±)-SdL19 (87.7 mg, quantitative). ¹H NMR (300 MHz, CDCl₃) δ: 7.50 (d, *J* = 2.5 Hz, H6'), 6.85 (t, *J* = 1.5 Hz, H3'), 6.10 (t, *J* = 1.5 Hz, H2'), 5.71 (d, *J* = 15.5 Hz, H7), 5.58 (dd, *J* = 7.5, 15.5 Hz, H6), 4.43 (t, *J* = 9.0 Hz, H5a), 4.07 (dd, *J* = 4.5, 9.0 Hz, H5b), 3.83-3.76 (m, H4), 1.99 (t, *J* = 1.5 Hz, 3 H7'), 1.29 (s, 3 H9 and 3 H10). ¹³C NMR (75 MHz, CDCl₃) δ: 171.4 (C2), 170.2 (C5'), 151.6 (C6'), 140.9 (C3'), 140.3 (C7), 135.8 (C4'), 123.7 (C6), 110.2 (C3), 100.6 (C2'), 71.2 (C5), 70.5 (C8), 39.3 (C4), 29.8 (C9 and C10), 10.7 (C7'). IR (cm⁻¹): 3460, 2973, 2924, 2850, 1783, 1750, 1682, 1372, 1345, 1265, 1185, 1089, 1032, 1010, 956, 863, 735, 703. HRMS (ESI): Calcd for C₁₅H₁₈O₆Na [M + Na]⁺: 317.1001, found: 317.0994.

911 **(2'R*,4R*)-SdL21**. To a solution of scandium trifluoromethanesulfonate (0.56 mg, 1.14 μmol) in CH₃CN (1.3 mL) was added silyl derivative (±)-SdL18F2 (83.5 mg, 0.33 mmol) in CH₃CN (0.29 mL) and water (2.0 μL, 0.11 μmol) at room temperature. The resultant mixture was stirred for 1 h at room temperature and quenched with a phosphate buffer (pH 7). The organic materials were extracted with dichloromethane (3 × 5 mL), the combined extracts were washed with brine, dried with Na₂SO₄, filtered and evaporated under reduced pressure to afford pure (±)-SdL21 (59.7 mg, 89%). ¹H NMR (300 MHz, CDCl₃) δ: 7.50 (d, *J* = 2.5 Hz, H6'), 6.89 (t, *J* = 1.5 Hz, H3'), 6.11 (t, *J* = 1.5 Hz, H2'), 5.68 (d, *J* = 15.5 Hz, H7), 5.54 (dd, *J* = 7.5, 15.5 Hz, H6), 4.43 (t, *J* = 9.0 Hz, H5a), 4.04 (dd, *J* = 4.5, 9.0 Hz, H5b), 3.82-3.74 (m, H4), 1.97 (t, *J* = 1.5 Hz, 3 H7'), 1.22 (s, 3 H9 and 3 H10). ¹³C NMR (75 MHz, CDCl₃) δ: 171.6 (C2), 170.4 (C5'), 151.7 (C6'), 141.1 (C3'), 140.7 (C7), 135.9 (C4'), 123.7 (C6), 110.6 (C3), 100.7 (C2'), 71.4 (C5), 70.7 (C8), 39.4 (C4), 29.9 (C9 and C10), 10.8 (C7'). IR

930 (cm⁻¹): 3488, 2969, 2925, 1784, 1751, 1682, 1343, 1263,
931 1185, 1084, 1026, 1013, 955, 863, 802, 730, 701. HRMS
932 (ESI): Calcd for C₁₅H₁₈O₆Na [M + Na]⁺: 317.1001, found:
933 317.1000. IR (cm⁻¹): 3488, 2969, 2925, 1784, 1751, 1682,
934 1343, 1263, 1185, 1084, 1026, 1013, 955, 863, 802, 730,
935 701. HRMS (ESI): Calcd for C₁₅H₁₈O₆Na [M + Na]⁺:
936 317.1001, found: 317.1000.

937 **(2'R*,4R*)-SdL33**. To a solution of (±)-SdL19 (15.6 mg,
938 0.05 mmol) in 0.3 mL of CH₂Cl₂ was added pyridine (0.09
939 mL, 1.06 mmol, 20 equiv), 4-nitrobenzoylchloride (49.2
940 mg, 0.26 mmol, 5 equiv) and DMAP (tip of spatula). The
941 mixture was stirred overnight at 40 °C. The mixture was
942 co-evaporated with toluene, extracted with EtOAc,
943 washed with NaHCO₃ and dried with Na₂SO₄, filtered and
944 evaporated under reduced pressure. The product was
945 purified by PTLC (heptane/EtOAc 60: 40) to afford pure
946 (±)-SdL33 (18.2 mg, 77%, yellow amorphous solid). ¹H
947 NMR (300 MHz, CDCl₃) δ: 8.26 (dt, *J* = 2.0, 8.5 Hz, H14 and
948 H14'), 8.11 (dt, *J* = 2.0, 8.5 Hz, H13 and H13'), 7.51 (d, *J* =
949 2.5 Hz, H6'), 6.89 (t, *J* = 1.5 Hz, H3'), 6.10 (t, *J* = 1.5 Hz,
950 H2'), 5.98 (dd, *J* = 1.0, 15.5 Hz, H7), 5.63 (q, *J* = 8.0 Hz, H6),
951 4.45 (t, *J* = 8.5 Hz, H5a), 4.10 (t, *J* = 7.5 Hz, H5b), 3.87-3.79
952 (m, H4), 2.02 (s, 3 H7'), 1.23 (t, *J* = 7.0 Hz, 3 H9 and 3
953 H10). ¹³C NMR (175 MHz, CDCl₃) δ: 171.4 (C2), 170.3
954 (C5'), 163.5 (C11), 151.8 (C6'), 150.6 (C15), 141.1 (C3'),
955 136.4 (C7), 131.5 (C4'), 130.7 (C13 and C13'), 126.8 (C6),
956 123.8 (C12), 123.7 (C14 and C14'), 110.0 (C3), 100.6
957 (C2'), 82.2 (C8), 71.2 (C5), 39.6 (C4), 27.3 (C9 or C10),
958 27.1 (C9 or C10), 11.0 (C7'). IR (cm⁻¹): 2919, 2850, 1785,
959 1755, 1722, 1683, 1607, 1527, 1464, 1349, 1290, 1185,
960 1102, 1033, 1014, 956, 876, 842, 720. HRMS (ESI): Calcd
961 for C₂₂H₂₁NO₉Na [M + Na]⁺: 466.1114, found: 466.1131.

962 **(2'R*,4S*)-SdL34**. To a solution of (±)-SdL21 (15.6 mg,
963 0.05 mmol) in 0.3 mL of CH₂Cl₂ was added pyridine (0.09
964 mL, 1.06 mmol, 20 equiv), 4-nitrobenzoylchloride (49.17
965 mg, 0.265 mmol, 5 equiv) and DMAP (tip of spatula). The
966 mixture was stirred overnight at 40 °C. The mixture was
967 co-evaporated with toluene, extracted with EtOAc,
968 washed with NaHCO₃ and dried with Na₂SO₄, filtered and
969 evaporated under reduced pressure. The product was
970 purified by PTLC (heptane/EtOAc 60: 40) to afford pure
971 (±)-SdL34 (6.8 mg, 25%, yellow amorphous solid). ¹H
972 NMR (300 MHz, CDCl₃) δ: 8.25 (dt, *J* = 2.0, 8.5 Hz, H14 and
973 H14'), 8.10 (dt, *J* = 2.0, 8.5 Hz, H13 and H13'), 7.50 (d, *J* =
974 2.5 Hz, H6'), 6.92 (t, *J* = 1.5 Hz, H3'), 6.11 (t, *J* = 1.5 Hz,
975 H2'), 5.96 (dd, *J* = 1.0, 15.5 Hz, H7), 5.60 (q, *J* = 8.0 Hz, H6),
976 4.46 (t, *J* = 8.5 Hz, H5a), 4.09 (t, *J* = 7.5 Hz, H5b), 3.87-3.79
977 (m, H4), 2.02 (s, 3 H7'), 1.24 (t, *J* = 7.0 Hz, 3 H9 and 3
978 H10). ¹³C NMR (175 MHz, CDCl₃) δ: 171.3 (C2), 170.3
979 (C5'), 163.5 (C11), 151.8 (C6'), 150.6 (C15), 141.2 (C3'),
980 136.6 (C7), 135.4 (C4'), 130.8 (C13 and C13'), 126.6 (C6),
981 125.2 (C12), 123.7 (C14 and C14'), 110.1 (C3), 100.7
982 (C2'), 82.2 (C8), 71.1 (C5), 39.7 (C4), 27.1 (C9 or C10),
983 27.0 (C9 or C10), 10.9 (C7'). IR (cm⁻¹): 2919, 2850, 1784,
984 1754, 1722, 1683, 1607, 1527, 1464, 1349, 1289, 1184,
985 1101, 1032, 1013, 955, 875, 842, 721. HRMS (ESI): Calcd
986 for C₂₄H₂₄N₂O₉Na [M + CH₃CN + Na]⁺: 507.1380, found:
987 507.1389.

988 **(2'R*,4S*)-SdL50**. To a solution of (±)-SdL21 (34.3 mg,
989 0.117 mmol) in CH₂Cl₂ (0.6 mL) was added pyridine
990 (0.189 mL, 2.34 mmol, 20 equiv), 3,5-dinitrobenzoyl chlo-

ride (134.9 mg, 0.58 mmol, 5 equiv) and DMAP (tip of
992 spatula). The mixture was stirred at 40 °C overnight. The
993 mixture was co-evaporated with toluene, extracted with
994 EtOAc, washed with NaHCO₃ and dried with Na₂SO₄. The
995 product was purified by PTLC (heptane/EtOAc 45: 55) to
996 afford pure (±)-SdL50 as a white solid (17.7 mg, 31%). ¹H
997 NMR (300 MHz, CDCl₃) δ: 9.19 (t, *J* = 2.0 Hz, H15), 9.04 (d,
998 *J* = 2.0 Hz, H13 and H13'), 7.52 (d, *J* = 2.5 Hz, H6'), 6.94 (t, *J* =
999 1.5 Hz, H3'), 6.12 (t, *J* = 1.5 Hz, H2'), 5.96 (dd, *J* = 1.0,
1000 16.0 Hz, H7), 5.65 (dd, *J* = 7.5, 15.5 Hz, H6), 4.46 (t, *J* = 9.0
1001 Hz, H5a), 4.08 (t, *J* = 5.0 Hz, H5b), 3.89-3.81 (m, H4), 2.02
1002 (s, 3 H7'), 1.65 (s, 3 H9 or 3 H10), 1.62 (s, 3 H9 or 3 H10).
1003 ¹³C NMR (125 MHz, CDCl₃) δ: 206.3 (C11), 171.2 (C5'),
1004 170.2 (C2), 152.0 (C6'), 148.8 (C12), 141.1 (C3'), 135.8
1005 (C7), 132.3 (C14 and C14'), 129.5 (C13 and C13'), 127.4
1006 (C6), 122.4 (C15), 109.9 (C4'), 100.9 (C2'), 71.1 (C8), 67.2
1007 (C5), 39.5 (C4), 29.9 (C3), 27.2 (C9 or C10), 26.8 (C9 or
1008 C10), 10.9 (C7'). R (cm⁻¹): 2985, 1737, 1447, 1373, 1301,
1009 1233, 1098, 1043, 938, 918, 847, 786. HRMS (ESI): Calcd
1010 for C₂₄H₂₃N₃O₁₁Na [M + CH₃CN + Na]⁺: 552.1230, found:
1011 552.1226.

1012 **(2'R*,4R*)-SdL51**. To a mixture of (±)-SdL19 (21.8 mg,
1013 0.07 mmol) and pyridine (250 μL, 3.09 mmol, 41.7 equiv)
1014 was added acetic anhydride (250 μL, 2.64 mmol, 35.7
1015 equiv) and DMAP (tip of spatula). The mixture was stirred
1016 at room temperature under argon overnight. The product
1017 was co-evaporated with toluene and purified by PTLC
1018 (heptane/EtOAc 45: 55) to afford pure (±)-SdL51 (10.2
1019 mg, 41%). ¹H NMR (300 MHz, CDCl₃) δ: 7.51 (d, *J* = 2.5 Hz,
1020 H6'), 6.95 (t, *J* = 1.5 Hz, H3'), 6.09 (t, *J* = 1.4 Hz, H2'), 5.83
1021 (dd, *J* = 1.0, 15.5 Hz, H7), 5.48 (dd, *J* = 8.0, 15.5 Hz, H6),
1022 4.43 (t, *J* = 8.5 Hz, H5a), 4.03 (t, *J* = 5.0 Hz, H5b), 3.83-3.74
1023 (m, H4), 1.95 (s, 3 H7'), 1.46 (d, *J* = 4.0 Hz, 3 H9 and 3
1024 H10), 1.23 (t, *J* = 7.0 Hz, 3 H12). ¹³C NMR (175 MHz,
1025 CDCl₃) δ: 171.4 (C11), 170.5 (C2), 170.0 (C5') 151.9 (C6'),
1026 141.4 (C3'), 137.3 (C7), 135.8 (C4'), 125.8 (C6), 109.7
1027 (C3), 100.7 (C2'), 80.0 (C8), 71.3 (C5), 39.6 (C4), 27.3 (C9
1028 or C10), 27.1 (C9 or C10), 14.4 (C12), 10.9 (C7'). IR (cm⁻¹):
1029 2985, 1737, 1447, 1373, 1301, 1234, 1097, 1043, 938,
1030 918, 847, 786. HRMS (ESI): Calcd for C₁₇H₂₀O₇Na [M +
1031 Na]⁺: 359.1107, found: 359.1109.

1032 **(2'R*,4R*)-SdL118F1 and (2'R*,4S*)-SdL118F2**. A mix-
1033 ture of compound **23b** (150.8 mg, 0.56 mmol), ethyl for-
1034 mate (0.09 mL, 1.12 mmol, 2 equiv) in THF (1.2 mL) was
1035 placed at -78°C. Potassium *tert*-butoxide was added
1036 (142.5 mg, 1.27 mmol, 2.26 equiv). The mixture was
1037 stirred during 2 h. A solution of bromide derivative **20**
1038 (106.2 mg, 0.60 mmol, 1.08 equiv) in THF (1.2 mL) was
1039 added. The mixture was stirred at room temperature for
1040 12 h. The mixture was diluted with EtOAc and saturated
1041 NH₄Cl aqueous solution. The organic phase was washed
1042 with water and brine. The combined organic layers were
1043 dried with Na₂SO₄, filtered and evaporated under reduced
1044 pressure. The mixture was purified by chromatography
1045 on silica gel (heptane/EtOAc 80: 20 to 70: 30 in 20 min)
1046 to afford pure products (±)-SdL118F1 and (±)-SdL118F2
1047 ((±)-SdL118F1: 52.3 mg (24%), (±)-SdL118F2: 66.3 mg
1048 (30%), total: 54%). (±)-SdL118F1: ¹H NMR (300 MHz,
1049 CDCl₃) δ: 7.51 (d, *J* = 2.5 Hz, H6'), 6.84 (quint, *J* = 1.5 Hz,
1050 H3'), 6.08 (dd, *J* = 1.0, 3.0 Hz, H2'), 5.52 (t, *J* = 5.5 Hz, H7
1051 and H6), 4.43 (td, *J* = 2.0, 15.5 Hz, H5a), 4.10 (q, *J* = 7.0 Hz,

1052 H5b), 3.81-3.74 (m, H4), 1.99 (t, $J = 1.5$ Hz, 3 H7'), 1.27 (s,
1053 3 H10), 0.91-0.82 (m, H9), 0.34-0.24 (m, 2 H11 and 2
1054 H12), 0.07 (s, 9 HTMS). ^{13}C NMR (75 MHz, CDCl_3) δ : 173.2
1055 (C2), 169.1 (C5'), 151.6 (C6'), 141.0 (C3'), 140.9 (C7),
1056 138.9 (C4'), 125.1 (C6), 110.1 (C3), 100.8 (C2'), 73.9 (C8),
1057 71.5 (C5), 39.7 (C4), 27.7 (C10), 22.6 (C9), 10.9 (C7'), 2.7
1058 (3C TMS), 1.5 (C11 and C12). IR (cm^{-1}): 2959, 1784, 1755,
1059 1684, 1346, 1249, 1185, 1093, 1019, 1028, 955, 863, 841,
1060 754. HRMS (ESI): Calcd for $\text{C}_{20}\text{H}_{28}\text{O}_6\text{SiNa}$ [$\text{M} + \text{Na}$] $^+$:
1061 415.1553, found: 415.1547. (\pm)-SdL118F2: ^1H NMR (300
1062 MHz, CDCl_3) δ : 7.51 (t, $J = 1.5$ Hz, H6'), 6.87 (sext, $J = 1.0$
1063 Hz, H3'), 6.09 (q, $J = 1.5$ Hz, H2'), 5.52-5.49 (m, H7 and
1064 H6), 4.43 (td, $J = 2.0, 15.5$ Hz, H5a), 4.03 (q, $J = 7.0$ Hz,
1065 H5b), 3.81-3.74 (m, H4), 1.97 (q, $J = 1.5$ Hz, 3 H7'), 1.23 (s,
1066 3 H10), 0.88-0.77 (m, H9), 0.28-0.21 (m, 2 H11 and 2
1067 H12), 0.05 (s, 9 HTMS). ^{13}C NMR (125 MHz, CDCl_3) δ :
1068 171.3 (C2), 170.2 (C5'), 151.3 (C6'), 141.0 (C3'), 140.9
1069 (C7), 134.8 (C4'), 126.7 (C6), 113.6 (C3), 100.5 (C2'), 74.3
1070 (C8), 71.5 (C5), 40.2 (C4), 29.9 (C10), 21.2 (C9), 10.9
1071 (C7'), 5.7 (3C TMS), 1.5 (C11 and C12). Carbonyl reso-
1072 nances are missing in ^{13}C NMR spectra of (\pm)-SdL118F1
1073 and (\pm)-SdL118F2 and found by HMBC spectra. IR (cm^{-1}):
1074 2969, 1784, 1760, 1685, 1346, 1248, 1185, 1086, 1030,
1075 1007, 956, 839, 750. HRMS (ESI): Calcd for $\text{C}_{20}\text{H}_{28}\text{O}_6\text{SiNa}$
1076 [$\text{M} + \text{Na}$] $^+$: 415.1553, found: 415.1540.

1077 **(2'R*,4R*)-SdL127**. To a solution of silyl ether (\pm)-
1078 SdL118F1 (23.0 mg, 0.06 mmol, 1 equiv) in CH_3CN (0.1
1079 mL), was added acetic anhydride (0.011 mL, 0.12 mmol, 2
1080 equiv) and scandium trifluoromethanesulfonate (0.29 mg,
1081 0.59 μmol) under argon. The mixture was stirred for 2 h
1082 at room temperature under argon. The mixture was purified
1083 by PTLC (heptane/EtOAc 40: 60) to afford pure alcohol
1084 (\pm)-SdL127 as a colorless oil (1.8 mg, 19%). ^1H NMR
1085 (300 MHz, CDCl_3) δ : 7.50 (t, $J = 3.0$ Hz, H6'), 6.87 (dt, $J =$
1086 1.5, 9.5 Hz, H3'), 6.09 (s, H2'), 5.62 (dq, $J = 3.5, 15.5$ Hz,
1087 H7), 5.51 (dd, $J = 7.0, 15.5$ Hz, H6), 4.43 (td, $J = 2.0, 9.0$ Hz,
1088 H5a), 4.05 (dd, $J = 4.0, 9.0$ Hz, H5b), 3.83-3.75 (m, H4),
1089 1.99 (s, 3 H7'), 1.28 (s, 3 H10), 0.89-82 (m, H9), 0.43-0.34
1090 (m, 2 H11 or 2 H12), 0.28-0.22 (m, 2 H11 or 2 H12). ^{13}C
1091 NMR (125 MHz, CDCl_3) δ : 171.5 (C2), 170.3 (C5'), 151.7
1092 (C6'), 141.0 (C3'), 137.6 (C6), 136.2 (C4'), 125.9 (C7),
1093 110.5 (C3), 100.8 (C2'), 72.0 (C8), 71.4 (C5), 39.7 (C4),
1094 28.1 (C10), 22.0 (C9), 10.9 (C7'), 1.5 (C11 or C12), 0.9
1095 (C11 or C12). IR (cm^{-1}): 3468, 2958, 2925, 2856, 1780,
1096 1745, 1680, 1459, 1369, 1344, 1263, 1183, 1083, 1029,
1097 1007, 953, 864, 798, 741, 672. HRMS (ESI): Calcd for
1098 $\text{C}_{17}\text{H}_{20}\text{O}_6\text{Na}$ [$\text{M} + \text{Na}$] $^+$: 347.1158, found: 347.1157.

1099 **X-ray Diffraction**. Thin colorless needle $0.30 \times 0.04 \times$
1100 0.03 mm was mounted on a nylon loop with protection
1101 Paratone® oil. Cell dimensions and intensities were
1102 measured at 203 K on a RIGAKU diffractometer constituted
1103 by a MM007 HF rotating-anode generator, delivering
1104 intense Cu(K α) radiation ($\lambda = 1.54187\text{\AA}$) through Osmic
1105 CMF confocal optics, and a Rapid II curved Image Plate
1106 detector allowing data measurement up to $2\theta_{\text{max}} = 144^\circ$;
1107 Clearly, the tiny crystals obtained by dissolving in ethyl
1108 acetate (48e)/ heptane (58e) and slow cooling of the
1109 solution turned out to be poor diffractors and a compro-
1110 mise was chosen between reasonable exposure time and
1111 exploitable data for model solution. 10732 measured
1112 reflections up to the θ value matching the *iUCR* criteria,

1113 4562 independent reflections ($R_{\text{int}} = 0.138$) of which
1114 only 687 had $|F_o| > 4\sigma(F_o)$ using the *CrystalClear 2.0*
1115 suite⁷⁵. Data were corrected for Lorentz and polarization
1116 effects and for absorption ($T_{\text{min, max}} : 0.448, 1.000$). De-
1117 spite the little signal detected beyond the 1.4\AA resolution
1118 limit, the structure could be readily solved either by dual
1119 methods (SHELXD)⁷⁶, or intrinsic phasing methods
1120 (*SHELXT* program⁷⁷; all other calculations regarding the
1121 model refinement were performed with *SHELXL* system⁷⁸
1122 and *PLATON*⁷⁹ programs, keeping meaningful X-ray diffrac-
1123 tion intensities. A potential solvent accessible region
1124 with disordered electron density was detected within the
1125 crystal structure. *SQUEEZE*⁸⁰ was used to model the unre-
1126 solved electron density likely resulting from disordered
1127 crystallizing solvent molecules, representing a total of 44
1128 electrons per unit cell. This contribution was not included
1129 in the crystal data. Full-matrix least-squares refinement
1130 based on F using the weight of $1/[\sigma^2(F_o) + 0.2(F_o^2)]$ gave
1131 final values of $R1 = 0.101$, $\omega R2 = 0.269$, and $\text{GOF}(F) =$
1132 1.241 for 319 parameters, 276 restraints on the thermal
1133 parameters for all the non-H atoms with the *SHELXL* RIGU
1134 command and 1012 contributing reflections. Maximum
1135 shift/error = 0.0000, max/min residual electron density =
1136 $0.283/-0.210 \text{ e.\AA}^{-3}$. Hydrogen atoms were placed in calcu-
1137 lated positions ($\text{C}-\text{H} = 0.94-1.00 \text{\AA}$) and refined as riding
1138 on their parent atoms, with $U_{\text{iso}}(\text{H})$ values constrained to
1139 $1.2 U_{\text{eq}}(\text{C})$ or $1.5 U_{\text{eq}}(\text{C}_{\text{methyl}})$. See Tables S1.

1140 **Plant material and growth conditions**. Pea (*Pisum sa-*
1141 *tivum*) branching mutants used in this study were derived
1142 from various cultivars of pea after ethyl methanesulfonate
1143 (EMS) mutagenesis and were described previously⁸¹. The
1144 *rms1-10* (M3T-884) and *rms3-4* (M2T-30) mutants were
1145 obtained from the dwarf cv Tèrese. Plants were grown in
1146 a greenhouse under long days as described in Braun et
1147 al.⁸².

1148 All *A. thaliana* plants used in this study originated from
1149 the Columbia (Col-0) ecotype background and have been
1150 described previously: *max3-11*⁶². Plants were grown as
1151 described in Cornet et al.⁸³ for a hydroponic assay (see
1152 also below).

1153 Two batches of parasitic plant seeds were used in this
1154 study. A population of seeds of *Phelipanche ramosa* (L.)
1155 Pomel associated to genetic group 1 (*P. ramosa* 1) was
1156 collected from Saint Martin-de-Fraigneau, France, on
1157 broomrape parasitizing winter oilseed rape (*Brassica*
1158 *napus* L.) in 2015. Seeds of *P. ramosa* from genetic sub-
1159 clade 2a (*P. ramosa* 2a) were harvested at Saint Martin-
1160 de-Bossenay, France, on broomrape developed on hemp
1161 (*Cannabis sativa* L.) in 2012³⁸. Seeds were surface steri-
1162 lized and conditioned according to Pouvreau et al.⁵⁷ (dark
1163 condition; 21°C).

1164 **Pea shoot branching assay**. The compounds to be tested
1165 were applied directly to the axillary bud with a micropi-
1166 pette as 10 μL of a solution containing 0.1% DMSO with
1167 2% polyethylene glycol 1450, 50% ethanol and 0.4%
1168 DMSO^{23,84}. The control-0 is the treatment with 0.1%
1169 DMSO without compound. 24 plants were sown per
1170 treatment in trays (2 repetitions of 12 plants). The treat-
1171 ment was generally performed 10 days after sowing, on
1172 the axillary bud at node 3. The branches at nodes 1 to 2
1173 were removed to encourage the outgrowth of axillary

1174 buds at nodes above. Nodes were numbered acropetally
1175 from the first scale leaf as node 1 and cotyledonary node
1176 as node 0. Bud growth at node 3 was measured with digi-
1177 tal callipers 8 to 10 days after treatment. Plants with a
1178 damaged main shoot apex or showing a dead white treat-
1179 ed-bud were excluded from the analysis. The SL-deficient
1180 *rms1-10* and SL-reception *rms3-4* pea mutants were used
1181 for all experiments and WT T r se was used as control.

1182 **Hydroponic assay on *Arabidopsis*.** The hydroponic
1183 assay was adapted from Cornet et al.⁸³. Seeds were sur-
1184 face-sterilized for 8 min in a solution of ethanol (95%)-
1185 Bayrochlore (Bayrol, Mundolsheim, France) (10%), and
1186 were rinsed twice with ethanol (100%). Each seed was
1187 sown on top of a cut 0.5 mL Eppendorf tube filled with
1188 agar medium containing 0.65% agar and 10% nutritive
1189 solution 5 mM NO₃. Tubes were soaked in water and
1190 stored in the dark at 4  C for 2 d. Twelve plants per pi-
1191 pette tip box (13 imes 9 imes 7 cm) were grown and supplied
1192 with nutrient solution as in Boyer et al.⁶⁰ at a concentra-
1193 tion of 5 mL.L⁻¹ (750 mL of solution per box). Every week
1194 the nutrient solution was renewed and every ten days
1195 when the molecules were added into the solution. The
1196 first treatment occurred at day 27 after sowing when
1197 plants started to bolt. The number of rosette branches
1198 was performed at day 42.

1199 **Germination stimulation activity assay on root para-
1200 sitic plant seeds.** Germination Stimulant activity (GS)
1201 of chemicals on seeds of parasitic plants were determined
1202 using a method described previously^{57,85}. Chemicals were
1203 suspended in DMSO, except all-*trans*- -carotene **17** in
1204 THF, at 10 mmol.L⁻¹, then diluted with water at 1 mmol.L⁻¹
1205 (water/DMSO; v/v; 9/1). Dilutions of 1 imes10⁻⁵ mol.L⁻¹ to
1206 1 imes10⁻¹² mol.L⁻¹ were then performed in water/DMSO
1207 (v/v; 9/1). For each compound, a range of concentrations
1208 from 10⁻¹³ to 10⁻⁶ mol.L⁻¹ (water/DMSO; 99/1) were ap-
1209 plied to conditioned parasitic seeds. DMSO 1% was used
1210 as negative control (seed germination < 1%) and ( )-
1211 GR24 at a concentration of 1  mol.L⁻¹ was used as a posi-
1212 tive control and induced 72-87% of seed germination for
1213 *P. ramosa* 1, 80–90% for *P. ramosa* 2a. To avoid variations
1214 related to sterilization events percentages of germination
1215 are reported as a ratio relative to the positive control
1216 (( )-GR24, 1  mol L⁻¹) included in each germination as-
1217 say. Each dilution and germination assay was repeated at
1218 least three times. For each compound tested, dose-
1219 response curves (Germination stimulation = f(c), Germi-
1220 nation Stimulant activity relative to ( )-GR24 1  mol L⁻¹ ;
1221 c : concentration (mol. L⁻¹), half maximal effective concen-
1222 tration (EC₅₀), and maximum of germination stimulant
1223 activity were determined using a Four Parameter Logistic
1224 Curve computed with SigmaPlot[ ] 10.0.

1225 **Fungal material.** *Rhizoglyphus irregularis* spores (strain
1226 DAOM197198) were purchased from Agronutrition
1227 (France). They were rinsed twice with sterile water be-
1228 fore use.

1229 **Analysis of hyphal branching *in vitro*.** Experiments
1230 were carried out as described in Taulera et al. (2020)⁶⁵.
1231 Spores were placed on plates containing M medium⁸⁶ and
1232 supplemented with SL analogs (100 nM.L⁻¹), or 0.1%
1233 DMSO for mock treatments. Plates were incubated at
1234 30  C under 2% CO₂ for 12 days. Germ tubes were then

1235 identified as the longest hypha coming out of each spore.
1236 The number of hyphal branches of the 1st order (growing
1237 from the germ tube) and higher order (growing from 1st-
1238 order branches) was scored using a dissecting micro-
1239 scope for each germinated spore. The average number of
1240 branches of each order was calculated for all the germi-
1241 nated spores on a plate (typically 25 to 35 spores). For
1242 statistical analysis, each plate was treated as a replication
1243 unit (represented by the plate mean), and 6 to 8 plates
1244 were analyzed for each treatment.

1245 **Symbiosis initiation assay.** The assay was carried out as
1246 described in Taulera et al.⁶⁵. Briefly, *ccd8-1* mutants of
1247 *Medicago truncatula*⁸⁷ were grown on a clay substrate
1248 inoculated with 150 spores of *R. irregularis*. SL analogs
1249 were added to the nutrient solution, to reach a final con-
1250 centration of 100 nM.L⁻¹. Mock treatments were per-
1251 formed with 0.1% DMSO. The number of infection points
1252 in each root system was recorded three weeks post-
1253 inoculation, after staining fungal structures with ink.

1254 **Expression and purification of proteins.** Expression
1255 and purification of proteins RMS3, AtD14, and PrKAI2d3
1256 with a cleavable GST tag were performed in accordance
1257 with de Saint Germain et al.^{51,61}.

1258 **Differential Scanning Fluorimetry (DSF).** DSF experi-
1259 ments were performed on a CFX384 TouchTM Real-Time
1260 PCR Detection System (Biorad) using excitation and emis-
1261 sion wavelengths of 490 and 575 nm, respectively. Sypro
1262 Orange ($\lambda_{Ex}/\lambda_{Em}$: 490/610 nm; Life technologies) was
1263 used as the reporter dye. Samples were heat-denatured
1264 using a linear 25 to 95  C gradient at a rate of 1.3  C per
1265 minute after incubation at 25  C for 30 min in the absence
1266 of light. The denaturation curve was obtained using CFX
1267 manager software. Final reaction mixtures were prepared
1268 in triplicate in 384-well white microplates, and each reac-
1269 tion was carried out in 20- L scale in PB buffer pH 6.8
1270 containing 10  g protein, each concentration of SL deriva-
1271 tives (DMSO solution, final DMSO concentration was 4%),
1272 and 0.008  L Sypro Orange. In the control reaction, DMSO
1273 was added instead of chemical solution.

1274 **NanoDSF.** Proteins were diluted in PBS (100 mM Phos-
1275 phate, pH 6.8, 150 mM NaCl) to a concentration of
1276 ~10  M. Ligands were tested at a concentration of
1277 200  M. The intrinsic fluorescence signal was measured
1278 as a function of increasing temperature with a Prome-
1279 theus NT.48 fluorimeter (NanoTemper Technologies),
1280 with 55% excitation light intensity and 1  C/min temper-
1281 ature ramp. Analyses were done on capillaries filled with
1282 10  L of the respective samples. Intrinsic fluorescence
1283 signals expressed by the 350 nm/330 nm emission ratio
1284 that increases as the proteins unfold, were plotted as a
1285 function of temperature (Figure 5A and Figure 5B). The
1286 plots show one of the three independent data collections
1287 performed for each protein.

1288 **Intrinsic tryptophan fluorescence assays and deter-
1289 mination of the dissociation constant K_D.** These experi-
1290 ments were performed as described previously in de
1291 Saint Germain et al.⁶¹ using a Spark Multimode Microplate
1292 Reader (Tecan).

1293 **Hydrolysis of ( )-SdL19 and ( )-GR24 in aqueous
1294 solution.** ( )-GR24 and ( )-SdL19 were tested for their

1295 chemical stability in an aqueous solution. Aqueous solu-
1296 tions of the compound to be tested (50 µg/mL) were
1297 incubated at 22 °C in the HPLC vials. The compounds
1298 were first dissolved in DMSO (2 mg/mL). Then, 25 µL of
1299 these solutions ((±)-GR24 and (±)-SdL19) were diluted to
1300 the final concentration with H₂O (750 µL) and EtOH (175
1301 µL) and the solution adjusted to pH 6.8. Aqueous solu-
1302 tions of the compounds to be tested (50 µg/mL) were
1303 incubated at 22 °C in the HPLC vials. (±)-1-Indanol (25 µL
1304 of a 1 mg/mL solution in DMSO) was added as internal
1305 standard to each solution. The samples were subjected to
1306 reverse-phase-ultra-performance liquid chromatography
1307 (RP-UPLC)-MS analyses by means of UPLC system
1308 equipped with a Photo Diode Array (PDA) and a Triple
1309 Quadrupole Detector (TQD) mass spectrometer (Acquity
1310 UPLC-TQD, Waters). RP-UPLC (HSS C₁₈ column, 1.8 µm,
1311 2.1 mm × 50 mm) with 0.1% (v/v) formic acid in CH₃CN
1312 and 0.1% (v/v) formic acid in water (aq. FA, 0.1%, v/v, pH
1313 2.8) as eluents [10% CH₃CN, followed by linear gradient
1314 from 10% to 100% of CH₃CN (4 min)] at a flow rate of
1315 0.6 mL.min⁻¹. The detection was done by PDA and with
1316 the TQD mass spectrometer operated in Electrospray
1317 ionization-positive mode at 3.2 kV capillary voltage. To
1318 maximize the signal, the cone voltage and collision energy
1319 were optimized to 20 V and 12 eV, respectively. The collision
1320 gas was argon at a pressure maintained near 4.5 10⁻³
1321 mBar. The relative quantity of remaining (non degraded)
1322 product was determined by integration in comparison
1323 with the internal standard.

1324 **Statistical analyses.** Because deviations from normality
1325 were observed for axillary bud length after SL treatment,
1326 the Kruskal-Wallis test was used to compare treatments
1327 using R Commander version 1.7–3⁸⁸. For bioassays with
1328 *Arabidopsis thaliana*, data were analyzed with the
1329 Shapiro-Wilkinson normality test. For bioassays with AM
1330 fungi, data were analyzed using Statgraphics Centurion
1331 software (SigmaPlus). Non-parametric tests were used
1332 because normality or homoscedasticity criteria were not
1333 met. Datasets were analyzed using the Kruskal-Wallis
1334 test, followed by pairwise comparisons with Mann-
1335 Whitney U test.

1336 ASSOCIATED CONTENT

1337 The Supporting Information is available free of charge at
1338 <https://pubs.acs.org/doi/xxx>. Crystallographic data of race-
1339 mic SdL50 (Table S1) and CIF file, bioactivity data (supple-
1340 mentary data for Figure 7, Tables S2-S3, Figure S1) and ¹H
1341 and ¹³C NMR spectra for the SdL compounds and precursors
1342 (**21**; **22a,b**; **23a,b**).

1343 AUTHOR INFORMATION

1344 Corresponding Author

1345 **François-Didier Boyer** – Université Paris-Saclay, CNRS,
1346 Institut de Chimie des Substances Naturelles, UPR 2301,
1347 91198, Gif-sur-Yvette, France; orcid.org/0000-0001-9855-
1348 7234; tel, ++33-1-69823017; Email [francois-
didier.boyer@cnrs.fr](mailto:francois-
1349 didier.boyer@cnrs.fr)

1350 Authors

1351 **Suzanne Daignan Fornier** – Université Paris-Saclay, CNRS,
1352 Institut de Chimie des Substances Naturelles, UPR 2301,
1353 91198, Gif-sur-Yvette, France; suzanne.daignan@cnrs.fr

1354 **Alexandre de Saint Germain** – Université Paris-Saclay,
1355 INRAE, AgroParisTech, Institut Jean-Pierre Bourgin (IJPB),
1356 78000, Versailles, France; [Alexandre.De-Saint-
Germain@inrae.fr](mailto:Alexandre.De-Saint-
1357 Germain@inrae.fr); orcid.org/0000-0003-2814-7234

1358 **Pascal Retailleau** – Université Paris-Saclay, CNRS, Institut
1359 de Chimie des Substances Naturelles, UPR 2301, 91198, Gif-
1360 sur-Yvette, France; pascal.retailleau@cnrs.fr; or-
1361 cid.org/0000-0003-3995-519X

1362 **Jean-Paul Pillot** – Université Paris-Saclay, INRAE, AgroPa-
1363 risTech, Institut Jean-Pierre Bourgin (IJPB), 78000, Ver-
1364 sailles, France; jean-paul.pillot@inrae.fr

1365 **Quentin Taulera** – Laboratoire de Recherche en Sciences
1366 Végétales, Université de Toulouse, CNRS, UPS, Toulouse INP,
1367 31320 Auzeville-Tolosane, France; [quentin.aulera@lrsv.ups-
tlse.fr](mailto:quentin.aulera@lrsv.ups-
1368 tlse.fr)

1369 **Lucile Andna** – Université de Strasbourg, Institut de Chimie,
1370 UMR 7177, Équipe Synthèse Organique et Phytochimie, 4 rue
1371 Blaise Pascal CS 90032, 67081 Strasbourg Cedex France;
1372 ljouffro@its.jnj.com; orcid.org/0000-0002-4185-9458

1373 **Laurence Miesch** – Université de Strasbourg, Institut de
1374 Chimie, UMR 7177, Équipe Synthèse Organique et Phytochi-
1375 mie, 4 rue Blaise Pascal CS 90032, 67081 Strasbourg Cedex
1376 France; lmiesch@unistra.fr; orcid.org/0000-0002-0369-
1377 9908

1378 **Soizic Rochange** – Laboratoire de Recherche en Sciences
1379 Végétales, Université de Toulouse, CNRS, UPS, Toulouse INP,
1380 31320 Auzeville-Tolosane, France; [rochange@lrsv.ups-
tlse.fr](mailto:rochange@lrsv.ups-
1381 tlse.fr); orcid.org/0000-0002-3889-7859

1382 **Jean-Bernard Pouvreau** – Nantes Université, CNRS, US2BN,
1383 UMR 6286, F-44000 Nantes, France; [Jean-
Bernard.Pouvreau@univ-nantes.fr](mailto:Jean-
1384 Bernard.Pouvreau@univ-nantes.fr); orcid.org/0000-0002-
1385 8351-9195

1386 Author Contributions

1387 F.-D.B. designed research; F.-D.B. and S.D.F. designed and
1388 synthesized the SdL analogs; L.A. and L.M. synthesized (±)-
1389 MeCLA; F.-D.B. performed the HPLC analyses; F.-D.B., J.-B.P.,
1390 J.-P.P., S.R. and Q.T. designed and performed the biological
1391 experiments; A.deS.G. performed the biochemical experi-
1392 ments. P.R. performed the X-ray analysis. All authors ana-
1393 lyzed the data; S.R. and F.-D.B. wrote the paper. All authors
1394 critically revised the manuscript and approved the submitted
1395 version.

1396 Funding Sources

1397 We are grateful to Hemp *it adn* for financial support. The IJPB
1398 benefits from the support of Saclay Plant Sciences-SPS (ANR-
1399 17-EUR-0007). This work has benefited from the support of
1400 IJPB's Plant Observatory technological platforms. A.d.S.G. has
1401 received the support of the EU in the framework of the Ma-
1402 rie-Curie FP7 COFUND People Programme, through the
1403 award of an AgreeSkills/AgreeSkills+ fellowship and the
1404 support of Saclay Plant Sciences-SPS (ANR-17-EUR-0007)
1405 through the award of a fellowship. The work of S.R. and Q.T.
1406 was supported by the TULIP LabEx (ANR-10-LABX-41). The
1407 CHARM3AT LabEx program (ANR-11-LABX-39) is also
1408 acknowledged for its support.

1410 Notes

1411 The authors declare no competing financial interest.

1412 ACKNOWLEDGMENT

1413 The authors thank Catherine Rameau for statistical analyses
1414 and Adrian Scaffidi for the generous gift of a sample of (±)-
1415 carlactone. The authors thank Jean-Marie Beau, Catherine

1416 Rameau and Sandrine Bonhomme for comments on the
1417 manuscript.

1418 REFERENCES

1419 1 Cook, C. E., Whichard, L. P., Turner, B. & Wall, M. E.
1420 Germination of Witchweed (*Striga Lutea* Lour) - Isolation
1421 and Properties of a Potent Stimulant. *Science* **154**, 1189-
1422 1190, doi:10.1126/science.154.3753.1189 (1966).

1423 2 Gomez-Roldan, V., Fermas, S., Brewer, P. B., Puech-Pages,
1424 V., Dun, E. A., Pillot, J.-P., Letisse, F., Matusova, R., Danoun,
1425 S., Portais, J.-C., Bouwmeester, H., Bécard, G., Beveridge, C.
1426 A., Rameau, C. & Rochange, S. F. Strigolactone inhibition of
1427 shoot branching. *Nature* **455**, 189-194,
1428 doi:10.1038/nature07271 (2008).

1429 3 Umehara, M., Hanada, A., Yoshida, S., Akiyama, K., Arite, T.,
1430 Takeda-Kamiya, N., Magome, H., Kamiya, Y., Shirasu, K.,
1431 Yoneyama, K., Kyojuzuka, J. & Yamaguchi, S. Inhibition of
1432 shoot branching by new terpenoid plant hormones.
1433 *Nature* **455**, 195-200, doi:10.1038/nature07272 (2008).

1434 4 Waters, M. T., Gutjahr, C., Bennett, T. & Nelson, D. C.
1435 Strigolactone Signaling and Evolution. *Annu. Rev. Plant*
1436 *Biol.* **68**, 291-322, doi:10.1146/annurev-arplant-042916-
1437 040925 (2017).

1438 5 Lopez-Obando, M., Ligerot, Y., Bonhomme, S., Boyer, F.-D.
1439 & Rameau, C. Strigolactone biosynthesis and signaling in
1440 plant development. *Development* **142**, 3615-3619,
1441 doi:10.1242/dev.120006 (2015).

1442 6 Yoneyama, K., Xie, X., Yoneyama, K., Kisugi, T., Nomura, T.,
1443 Nakatani, Y., Akiyama, K. & McErlean, C. S. P. Which are the
1444 major players, canonical or non-canonical strigolactones?
1445 *J. Exp. Bot.* **69**, 2231-2239, doi:10.1093/jxb/ery090
1446 (2018).

1447 7 Wakabayashi, T., Hamana, M., Mori, A., Akiyama, R., Ueno,
1448 K., Osakabe, K., Osakabe, Y., Suzuki, H., Takikawa, H.,
1449 Mizutani, M. & Sugimoto, Y. Direct conversion of
1450 carlactonoic acid to orobanchol by cytochrome P450
1451 CYP722C in strigolactone biosynthesis. *Sci. Adv.* **5**,
1452 eaax9067, doi:10.1126/sciadv.aax9067 (2019).

1453 8 Wakabayashi, T., Shida, K., Kitano, Y., Takikawa, H.,
1454 Mizutani, M. & Sugimoto, Y. CYP722C from *Gossypium*
1455 *arboreum* catalyzes the conversion of carlactonoic acid to
1456 5-deoxystrigol. *Planta* **251**, 97, doi:10.1007/s00425-020-
1457 03390-6 (2020).

1458 9 Mori, N., Sado, A., Xie, X., Yoneyama, K., Asami, K., Seto, Y.,
1459 Nomura, T., Yamaguchi, S., Yoneyama, K. & Akiyama, K.
1460 Chemical identification of 18-hydroxycarlactonoic acid as
1461 an LjMAX1 product and *in planta* conversion of its methyl
1462 ester to canonical and non-canonical strigolactones in
1463 *Lotus japonicus*. *Phytochemistry* **174**, 112349,
1464 doi:10.1016/j.phytochem.2020.112349 (2020).

1465 10 Wang, J. Y., Lin, P.-Y. & Al-Babili, S. On the biosynthesis and
1466 evolution of apocarotenoid plant growth regulators.
1467 *Seminars in Cell & Developmental Biology* **109**, 3-11,
1468 doi:10.1016/j.semcdb.2020.07.007 (2021).

1469 11 Yoda, A., Mori, N., Akiyama, K., Kikuchi, M., Xie, X., Miura,
1470 K., Yoneyama, K., Sato-Izawa, K., Yamaguchi, S., Yoneyama,
1471 K., Nelson, D. C. & Nomura, T. Strigolactone biosynthesis
1472 catalyzed by cytochrome P450 and sulfotransferase in
1473 sorghum. *New Phytol.* **232**, 1999-2010,
1474 doi:10.1111/nph.17737 (2021).

1475 12 Brewer, P. B., Yoneyama, K., Filardo, F., Meyers, E., Scaffidi,
1476 A., Frickey, T., Akiyama, K., Seto, Y., Dun, E. A., Cremer, J. E.,
1477 Kerr, S. C., Waters, M. T., Flematti, G. R., Mason, M. G.,
1478 Weiller, G., Yamaguchi, S., Nomura, T., Smith, S. M. &
1479 Beveridge, C. A. LATERAL BRANCHING OXIDOREDUCTASE
1480 acts in the final stages of strigolactone biosynthesis in
1481 *Arabidopsis*. *Proc. Natl. Acad. Sci. U.S.A.* **113**, 6301-6306,
1482 doi:10.1073/pnas.1601729113 (2016).

1483 13 Yoneyama, K., Akiyama, K., Brewer, P. B., Mori, N.,
1484 Kawano-Kawada, M., Haruta, S., Nishiwaki, H., Yamauchi,
1485 S., Xie, X., Umehara, M., Beveridge, C. A., Yoneyama, K. &
1486 Nomura, T. Hydroxyl carlactone derivatives are

1487 predominant strigolactones in *Arabidopsis*. *Plant Direct* **4**,
1488 e00219, doi:10.1002/pld3.219 (2020).

1489 14 Yoneyama, K. Recent progress in the chemistry and
1490 biochemistry of strigolactones. *J. Pestic. Sci.* **45**, 45-53,
1491 doi:10.1584/jpestics.D19-084 (2020).

1492 15 Bromhead, L. J. & McErlean, C. S. P. Accessing Single
1493 Enantiomer Strigolactones: Progress and Opportunities.
1494 *Eur. J. Org. Chem.*, 5712-5723,
1495 doi:10.1002/ejoc.201700865 (2017).

1496 16 Yasui, M., Ota, R., Tsukano, C. & Takemoto, Y. Total
1497 synthesis of avenaol. *Nat. Commun.* **8**, 674,
1498 doi:10.1038/s41467-017-00792-1 (2017).

1499 17 Yasui, M., Yamada, A., Tsukano, C., Hamza, A., Pápai, I. &
1500 Takemoto, Y. Enantioselective Acetalization by Dynamic
1501 Kinetic Resolution for the Synthesis of γ -
1502 Alkoxybutenolides by Thiourea/Quaternary Ammonium
1503 Salt Catalysts: Application to Strigolactones. *Angew. Chem.*
1504 *Int. Ed.* **59**, 13479-13483, doi:10.1002/anie.202002129
1505 (2020).

1506 18 Yoshimura, M., Dieckmann, M., Dakas, P.-Y., Fonné-Pfister,
1507 R., Screpanti, C., Hermann, K., Rendine, S., Quinodoz, P.,
1508 Horoz, B., Catak, S. & De Mesmaeker, A. Total Synthesis
1509 and Biological Evaluation of Zealactone 1a/b. *Helv. Chim.*
1510 *Acta* **103**, e2000017, doi:10.1002/hlca.202000017
1511 (2020).

1512 19 Takahashi, I. & Asami, T. Target-based selectivity of
1513 strigolactone agonists and antagonists in plants and their
1514 potential use in agriculture. *J. Exp. Bot.* **69**, 2241-2254,
1515 doi:10.1093/jxb/ery126 (2018).

1516 20 Jamil, M., Kountche, B. A. & Al-Babili, S. Current progress in
1517 *Striga* management. *Plant Physiol.* **185**, 1339-1352,
1518 doi:10.1093/plphys/kiab040 (2021).

1519 21 Johnson, A. W., Gowda, G., Hassanali, A., Knox, J., Monaco,
1520 S., Razavi, Z. & Rosebery, G. The Preparation of Synthetic
1521 Analogs of Strigol. *J. Chem. Soc., Perkin Trans. 1*, 1734-
1522 1743, doi:10.1039/P19810001734 (1981).

1523 22 Kodama, K., Rich, M. K., Yoda, A., Shimazaki, S., Xie, X.,
1524 Akiyama, K., Mizuno, Y., Komatsu, A., Luo, Y., Suzuki, H.,
1525 Kameoka, H., Libourel, C., Keller, J., Sakakibara, K.,
1526 Nishiyama, T., Nakagawa, T., Mashiguchi, K., Uchida, K.,
1527 Yoneyama, K., Tanaka, Y., Yamaguchi, S., Shimamura, M.,
1528 Delaux, P.-M., Nomura, T. & Kyojuzuka, J. An Ancestral
1529 Function of Strigolactones as Symbiotic Rhizosphere
1530 Signals. *bioRxiv*, doi:10.1101/2021.08.20.457034 (2021).

1531 23 Boyer, F.-D., de Saint Germain, A., Pillot, J.-P., Pouvreau, J.-
1532 B., Chen, V. X., Ramos, S., Stévenin, A., Simier, P., Delavault,
1533 P., Beau, J.-M. & Rameau, C. Structure-Activity Relationship
1534 Studies of Strigolactone-Related Molecules for Branching
1535 Inhibition in Garden Pea: Molecule Design for Shoot
1536 Branching. *Plant Physiol.* **159**, 1524-1544,
1537 doi:10.1104/pp.112.195826 (2012).

1538 24 Umehara, M., Cao, M., Akiyama, K., Akatsu, T., Seto, Y.,
1539 Hanada, A., Li, W., Takeda-Kamiya, N., Morimoto, Y. &
1540 Yamaguchi, S. Structural Requirements of Strigolactones
1541 for Shoot Branching Inhibition in Rice and *Arabidopsis*.
1542 *Plant Cell Physiol.* **56**, 1059-1072,
1543 doi:10.1093/pcp/pcv028 (2015).

1544 25 Xie, X., Yoneyama, K. & Yoneyama, K. The Strigolactone
1545 Story. *Annu. Rev. Phytopathol.* **48**, 93-117,
1546 doi:10.1146/annurev-phyto-073009-114453 (2010).

1547 26 Mori, N., Nishiuma, K., Sugiyama, T., Hayashi, H. &
1548 Akiyama, K. Carlactone-type strigolactones and their
1549 synthetic analogues as inducers of hyphal branching in
1550 arbuscular mycorrhizal fungi. *Phytochemistry* **130**, 90-98,
1551 doi:10.1016/j.phytochem.2016.05.012 (2016).

1552 27 Jamil, M., Kountche, B. A., Wang, J. Y., Haider, I., Jia, K. P.,
1553 Takahashi, I., Ota, T., Asami, T. & Al-Babili, S. A New Series
1554 of Carlactonoic Acid Based Strigolactone Analogs for
1555 Fundamental and Applied Research. *Front. Plant Sci.* **11**,
1556 434, doi:10.3389/fpls.2020.00434 (2020).

1557 28 Jamil, M., Kountche, B. A., Haider, I., Guo, X., Ntui, V. O., Jia,
1558 K.-P., Ali, S., Hameed, U. S., Nakamura, H., Lyu, Y., Jiang, K.,
1559 Hirabayashi, K., Tanokura, M., Arold, S. T., Asami, T. & Al-
1560 Babili, S. Methyl phenlactonoates are efficient

- 1561 strigolactone analogs with simple structure. *J. Exp. Bot.* **69**, 1635
1562 2319-2331, doi:10.1093/jxb/erx438 (2018). 1636
- 1563 29 Parker, C. Parasitic Weeds: A World Challenge. *Weed Sci.* 1637
1564 **60**, 269-276, doi:10.1614/WS-D-11-00068.1 (2012). 1638
- 1565 30 Grenz, J. H. & Sauerborn, J. Mechanisms limiting the 1639
1566 geographical range of the parasitic weed *Orobanch* 1640
1567 *crenata*. *Agric. Ecosyst. Environ.* **122**, 275-281, 1641
1568 doi:10.1016/j.agee.2007.01.014 (2007). 1642
- 1569 31 Delavault, P., Montiel, G., Brun, G., Pouvreau, J. B., Thoiron, 1643
1570 S. & Simier, P. Communication Between Host Plants and 1644
1571 Parasitic Plants. *Adv. Bot. Res.* **82**, 55-82, 1645
1572 doi:10.1016/bs.abr.2016.10.006 (2017). 1646
- 1573 32 Brun, G., Spallek, T., Simier, P. & Delavault, P. Molecular 1647
1574 actors of seed germination and haustoriogenesis in 1648
1575 parasitic weeds. *Plant Physiol.* **185**, 1270-1281, 1649
1576 doi:10.1093/plphys/kiab041 (2021). 1650
- 1577 33 Fernandez-Aparicio, M., Reboud, X. & Gibot-Leclerc, S. 1651
1578 Broomrape Weeds. Underground Mechanisms of 1652
1579 Parasitism and Associated Strategies for their Control: A 1653
1580 Review. *Front. Plant Sci.* **7**, 135, 1654
1581 doi:10.3389/fpls.2016.00135 (2016). 1655
- 1582 34 Akiyama, K., Matsuzaki, K. & Hayashi, H. Plant 1656
1583 sesquiterpenes induce hyphal branching in arbuscular 1657
1584 mycorrhizal fungi. *Nature* **435**, 824-827, 1658
1585 doi:10.1038/nature03608 (2005). 1659
- 1586 35 Besserer, A., Puech-Pages, V., Kiefer, P., Gomez-Roldan, V., 1660
1587 Jauneau, A., Roy, S., Portais, J. C., Roux, C., Bécard, G. & 1661
1588 Sejalon-Delmas, N. Strigolactones stimulate arbuscular 1662
1589 mycorrhizal fungi by activating mitochondria. *PLoS Biol.* **4**, 1663
1590 1239-1247, doi:e226 (2006). 1664
- 1591 36 Besserer, A., Bécard, G., Jauneau, A., Roux, C. & Sejalon- 1665
1592 Delmas, N. GR24, a synthetic analog of strigolactones, 1666
1593 stimulates the mitosis and growth of the arbuscular 1667
1594 mycorrhizal fungus *Gigaspora rosea* by boosting its energy 1668
1595 metabolism. *Plant Physiol.* **148**, 402-413, 1669
1596 doi:10.1104/pp.108.121400 (2008). 1670
- 1597 37 Rich, M. K., Vigneron, N., Libourel, C., Keller, J., Xue, L., 1671
1598 Hajheidari, M., Radhakrishnan Guru, V., Le Ru, A., Diop 1672
1599 Seydina, I., Potente, G., Conti, E., Duijsings, D., Batut, A., Le 1673
1600 Faouder, P., Kodama, K., Kyoizuka, J., Sallet, E., Bécard, G., 1674
1601 Rodriguez-Franco, M., Ott, T., Bertrand-Michel, J., Oldroyd 1675
1602 Giles, E. D., Szóvényi, P., Bucher, M. & Delaux, P.-M. Lipid 1676
1603 exchanges drove the evolution of mutualism during plant 1677
1604 terrestrialization. *Science* **372**, 864-868, 1678
1605 doi:10.1126/science.abg0929 (2021). 1679
- 1606 38 Stojanova, B., Delourme, R., Duffé, P., Delavault, P. & 1680
1607 Simier, P. Genetic differentiation and host preference 1681
1608 reveal non-exclusive host races in the generalist parasitic 1682
1609 weed *Phelipanche ramosa*. *Weed Res.* **59**, 107-118, 1683
1610 doi:10.1111/wre.12353 (2019). 1684
- 1611 39 Huet, S., Pouvreau, J.-B., Delage, E., Delgrange, S., Marais, 1685
1612 C., Bahut, M., Delavault, P., Simier, P. & Poulin, L. 1686
1613 Populations of the Parasitic Plant *Phelipanche ramosa* 1687
1614 Influence Their Seed Microbiota. *Front. Plant Sci.* **11**, 1075, 1688
1615 doi:10.3389/fpls.2020.01075 (2020). 1689
- 1616 40 Auger, B., Pouvreau, J.-B., Pouponneau, K., Yoneyama, K., 1690
1617 Montiel, G., Le Bizec, B., Yoneyama, K., Delavault, P., 1691
1618 Delourme, R. & Simier, P. Germination Stimulants of 1692
1619 *Phelipanche ramosa* in the Rhizosphere of *Brassica napus* 1693
1620 Are Derived from the Glucosinolate Pathway. *Mol. Plant- 1694
1621 Microbe Interact.* **25**, 993-1004, doi:10.1094/mpmi-01- 1695
1622 12-0006-r (2012). 1696
- 1623 41 Xie, X., Kusumoto, D., Takeuchi, Y., Yoneyama, K., Yamada, 1697
1624 Y. & Yoneyama, K. 2'-Epi-orobanchol and solanacol, two 1698
1625 unique strigolactones, germination stimulants for root 1699
1626 parasitic weeds, produced by tobacco. *J. Agric. Food. Chem.* 1700
1627 **55**, 8067-8072, doi:10.1021/jf0715121 (2007). 1701
- 1628 42 Xie, X., Yoneyama, K., Kisugi, T., Uchida, K., Ito, S., Akiyama, 1702
1629 K., Hayashi, H., Yokota, T., Nomura, T. & Yoneyama, K. 1703
1630 Confirming Stereochemical Structures of Strigolactones 1704
1631 Produced by Rice and Tobacco. *Mol. Plant* **6**, 153-163, 1705
1632 doi:10.1093/mp/sss139 (2013). 1706
- 1633 43 Koltai, H., Cohen, M., Chesin, O., Mayzlish-Gati, E., Bécard, 1707
1634 G., Puech, V., Ben Dor, B., Resnick, N., Winger, S. &
- Kapulnik, Y. Light is a positive regulator of strigolactone 1708
1709 levels in tomato roots. *J. Plant Physiol.* **168**, 1993-1996, 1710
1711 doi:10.1016/j.jplph.2011.05.022 (2011). 1712
- 44 Hamzaoui, O., Maciuk, A., Delgrange, S., Kerdja, K., 1713
1714 Thouminot, C., Germain, A. d. S., Rochange, S., Boyer, F.-D., 1715
1716 Simier, P. & Pouvreau, J.-B. Cannalactone: a new non- 1717
1718 canonical strigolactone exudated by *Cannabis sativa* roots 1719
1720 with a pivotal role in host specialization within French 1721
1722 broomrape (*Phelipanche ramosa*) populations in 15th 1723
1724 World Congress on Parasitic Plants. (Amsterdam, 2019). 1725
- 45 de Saint Germain, A., Retailleau, P., Norsikian, S., 1726
1727 Servajean, V., Pelissier, F., Steinmetz, V., Pillot, J.-P., 1728
1729 Rochange, S., Pouvreau, J.-B. & Boyer, F.-D. Contalactone, a 1730
1731 contaminant formed during chemical synthesis of the 1732
1732 strigolactone reference GR24 is also a strigolactone mimic. 1733
1733 *Phytochemistry* **168**, 112112, 1734
1734 doi:10.1016/j.phytochem.2019.112112 (2019). 1735
- 46 Hamiaux, C., Drummond, R. S. M., Janssen, B. J., Ledger, S. 1736
1737 E., Cooney, J. M., Newcomb, R. D. & Snowden, K. C. DAD2 Is 1738
1739 an α/β Hydrolase Likely to Be Involved in the Perception 1739
1740 of the Plant Branching Hormone, Strigolactone. *Curr. Biol.* 1740
1741 **22**, 2032-2036, doi:10.1016/j.cub.2012.08.007 (2012). 1741
- 47 Waters, M. T., Nelson, D. C., Scaffidi, A., Flematti, G. R., Sun, 1742
1743 Y. K., Dixon, K. W. & Smith, S. M. Specialisation within the 1743
1744 DWARF14 protein family confers distinct responses to 1744
1745 karrikins and strigolactones in *Arabidopsis*. *Development* 1745
1746 **139**, 1285-1295, doi:10.1242/dev.074567 (2012). 1746
- 48 Conn, C. E., Bythell-Douglas, R., Neumann, D., Yoshida, S., 1747
1748 Whittington, B., Westwood, J. H., Shirasu, K., Bond, C. S., 1748
1749 Dyer, K. A. & Nelson, D. C. Convergent evolution of 1749
1750 strigolactone perception enabled host detection in 1750
1751 parasitic plants. *Science* **349**, 540-543, 1751
1752 doi:10.1126/science.aab1140 (2015). 1752
- 49 Toh, S., Holbrook-Smith, D., Stogios, P. J., Onopriyenko, O., 1753
1754 Lumba, S., Tsuchiya, Y., Savchenko, A. & McCourt, P. 1754
1755 Structure-function analysis identifies highly sensitive 1755
1756 strigolactone receptors in *Striga*. *Science* **350**, 203-207, 1756
1757 doi:10.1126/science.aac9476 (2015). 1757
- 50 Nelson, D. C. The mechanism of host-induced germination in 1758
1759 root parasitic plants. *Plant Physiol.* **185**, 1353-1373, 1759
1760 doi:10.1093/plphys/kiab043 (2021). 1760
- 51 de Saint Germain, A., Jacobs, A., Brun, G., Pouvreau, J.-B., 1761
1762 Braem, L., Cornu, D., Clavé, G., Baudu, E., Steinmetz, V., 1762
1763 Servajean, V., Wicke, S., Gevaert, K., Simier, P., 1763
1764 Goomachtig, S., Delavault, P. & Boyer, F.-D. A *Phelipanche* 1764
1765 *ramosa* KAI2 protein perceives strigolactones and 1765
1766 isothiocyanates enzymatically. *Plant Commun.* **2**, 100166, 1766
1767 doi:10.1016/j.xplc.2021.100166 (2021). 1767
- 52 Křižková, P. M., Lindner, W. & Hammerschmidt, F. 1768
1769 Improved Synthesis of Racemate and Enantiomers of 1769
1770 Taniguchi Lactone and Conversion of Their C-C Double 1770
1771 Bonds into Triple Bonds. *Synthesis* **50**, 651-657, 1771
1772 doi:10.1055/s-0036-1591516 (2018). 1772
- 53 Ballini, R., Marcantoni, E. & Perella, S. A Two Steps 1773
1774 Synthesis of γ -Substituted and γ,γ -Disubstituted α - 1773
1775 (Alkylmethylene)- γ -butyrolactones. *J. Org. Chem.* **64**, 1774
1776 2954-2957, doi:10.1021/jo982131c (1999). 1775
- 54 Bartoli, G., Marcantoni, E. & Petrini, M. CeCl₃-Mediated 1776
1777 Addition of Grignard Reagents to 1,3-Diketones. *Angew.* 1777
1778 *Chem. Int. Ed.* **32**, 1061-1062, 1778
1779 doi:10.1002/anie.199310611 (1993). 1779
- 55 Oriyama, T., Kobayashi, Y. & Noda, K. Chemoselective and 1780
1781 Practical Deprotection of Alkyl Trialkylsilyl Ethers in the 1780
1782 Presence of Aryl Trialkylsilyl Ethers by a Catalytic Amount 1781
1783 of Sc(OTf)₃. *Synlett*, 1047-1048, doi:10.1055/s-1998-1890 1782
1784 (1998). 1783
- 56 Norsikian, S., Holmes, I., Lagasse, F. & Kagan, H. B. A one- 1784
1785 pot esterification of chiral *O*-trimethylsilyl-cyanohydrins 1785
1786 with retention of stereochemistry. *Tetrahedron Lett.* **43**, 1786
1787 5715-5717, doi:10.1016/S0040-4039(02)01200-5 1787
1788 (2002). 1788
- 57 Pouvreau, J. B., Gaudin, Z., Auger, B., Lechat, M. M., 1789
1790 Gauthier, M., Delavault, P. & Simier, P. A high-throughput 1790

- 1708 seed germination assay for root parasitic plants. *Plant* 1781 70 Scaffidi, A., Waters, M. T., Ghisalberti, E. L., Dixon, K. W.,
1709 *Methods* **9**, 32, doi:10.1186/1746-4811-9-32 (2013). 1782 Flematti, G. R. & Smith, S. M. Carlactone-independent
1710 58 Miura, H., Ochi, R., Nishiwaki, H., Yamauchi, S., Xie, X., 1783 seedling morphogenesis in Arabidopsis. *Plant J.* **76**, 1-9,
1711 Nakamura, H., Yoneyama, K. & Yoneyama, K. Germination 1784 doi:10.1111/tj.12265 (2013).
1712 Stimulant Activity of Isothiocyanates on *Phelipanche* spp. 1785 71 Boutet-Mercey, S., Perreau, F., Roux, A., Clavé, G., Pillot, J.-
1713 *Plants* **11**, 606, doi:10.3390/plants11050606 (2022). 1786 P., Schmitz-Afonso, I., Touboul, D., Mouille, G., Rameau, C.
1714 59 Boyer, F.-D., de Saint Germain, A., Pillot, J. P., Pouvreau, J.- 1787 & Boyer, F.-D. Validated Method for Strigolactone
1715 B., Chen, V. X., Ramos, S., Stevenin, A., Simier, P., Delavault, 1788 Quantification by Ultra High-Performance Liquid
1716 P., Beau, J.-M. & Rameau, C. Structure-activity relationship 1789 Chromatography – Electrospray Ionisation Tandem Mass
1717 studies of strigolactone-related molecules for branching 1790 Spectrometry Using Novel Deuterium Labelled Standards.
1718 inhibition in garden pea: molecule design for shoot 1791 *Phytochem. Anal.* **29**, 59-68, doi:10.1002/pca.2714 (2018).
1719 branching. *Plant Physiol.* **159**, 1524-1544, 1792 Chen, V. X., Boyer, F.-D., Rameau, C., Pillot, J.-P., Vors, J.-P. &
1720 doi:10.1104/pp.112.195826 (2012). 1793 Chen, J.-M. New Synthesis of A-Ring Aromatic
1721 60 Boyer, F.-D., de Saint Germain, A., Pouvreau, J.-B., Clavé, G., 1794 Strigolactone Analogues and Their Evaluation as Plant
1722 Pillot, J.-P., Roux, A., Rasmussen, A., Depuydt, S., 1795 Hormones in Pea (*Pisum sativum*). *Chem. – Eur. J.* **19**,
1723 Lauressergues, D., Frei dit Frey, N., Heugebaert, T. S. A., 1796 4849-4857, doi:10.1002/chem.201203585 (2013).
1724 Stevens, C. V., Geelen, D., Goormachtig, S. & Rameau, C. 1797 73 Macalpine, G. A., Raphael, R. A., Shaw, A., Taylor, A. W. &
1725 New Strigolactone Analogs as Plant Hormones with Low 1798 Wild, H. J. Synthesis of Germination Stimulant (±)-Strigol.
1726 Activities in the Rhizosphere. *Mol. Plant* **7**, 675-690, 1799 *J. Chem. Soc., Perkin Trans. 1*, 410-416,
1727 doi:10.1093/mp/sst163 (2014). 1800 doi:10.1039/C39740000834 (1976).
1728 61 de Saint Germain, A., Clavé, G., Badet-Denisot, M.-A., Pillot, 1801 74 Sugano, G., Kawada, K., Shigeta, M., Hata, T. & Urabe, H.
1729 J.-P., Cornu, D., Le Caer, J.-P., Burger, M., Pelissier, F., 1802 Iron-catalyzed δ -selective conjugate addition of methyl
1730 Retailleau, P., Turnbull, C., Bonhomme, S., Chory, J., 1803 and cyclopropyl Grignard reagents to $\alpha,\beta,\gamma,\delta$ -unsaturated
1731 Rameau, C. & Boyer, F.-D. An histidine covalent receptor 1804 esters and amides. *Tetrahedron Lett.* **60**, 885-890,
1732 and butenolide complex mediates strigolactone 1805 doi:10.1016/j.tetlet.2018.12.043 (2019).
1733 perception. *Nat. Chem. Biol.* **12**, 787-794, 1806 Rigaku, O. D. CrystalClear-SM Expert 2.0 r4 Rigaku
1734 doi:10.1038/nchembio.2147 (2016). 1807 Corporation, Tokyo, Japan. (2009).
1735 62 Auldridge, M. E., Block, A., Vogel, J. T., Dabney-Smith, C., 1808 76 Schneider, T. R. & Sheldrick, G. M. Substructure solution
1736 Mila, I., Bouzayen, M., Magallanes-Lundback, M., 1809 with SHELXD. *Acta Crystallogr., Sect. D: Biol. Crystallogr.*
1737 DellaPenna, D., McCarty, D. R. & Klee, H. J. Characterization 1810 **58**, 1772-1779, doi:doi:10.1107/S0907444902011678
1738 of three members of the Arabidopsis carotenoid cleavage 1811 (2002).
1739 dioxygenase family demonstrates the divergent roles of 1812 Sheldrick, G. M. Crystal structure refinement with SHELXL.
1740 this multifunctional enzyme family. *Plant J.* **45**, 982-993, 1813 *Acta Crystallogr., Sect. C: Cryst. Struct. Commun.* **71**, 3-8,
1741 doi:10.1111/j.1365-313X.2006.02666.x (2006). 1814 doi:10.1107/s2053229614024218 (2015).
1742 63 Xie, X. Structural diversity of strigolactones and their 1815 78 Sheldrick, G. M. SHELXT - Integrated space-group and
1743 distribution in the plant kingdom. *J. Pestic. Sci.* **41**, 175- 1816 crystal-structure determination. *Acta Crystallogr., Sect. A:*
1744 180, doi:10.1584/jpestics.J16-02 (2016). 1817 *Found. Crystallogr.* **71**, 3-8,
1745 64 Akiyama, K., Ogasawara, S., Ito, S. & Hayashi, H. Structural 1818 doi:10.1107/s2053273314026370 (2015).
1746 Requirements of Strigolactones for Hyphal Branching in 1819 79 Spek, A. L. Structure validation in chemical
1747 AM Fungi. *Plant Cell Physiol.* **51**, 1104-1117, 1820 crystallography. *Acta Crystallogr., Sect. D: Biol. Crystallogr.*
1748 doi:10.1093/pcp/pcq058 (2010). 1821 **65**, 148-155, doi:10.1107/s090744490804362x (2009).
1749 65 Taulera, Q., Lauressergues, D., Martin, K., Cadoret, M., 1822 80 Spek, A. L. PLATONSQUEEZE: a tool for the calculation of
1750 Servajean, V., Boyer, F.-D. & Rochange, S. Initiation of 1823 the disordered solvent contribution to the calculated
1751 arbuscular mycorrhizal symbiosis involves a novel 1824 structure factors. *Acta Crystallogr., Sect. C: Cryst. Struct.*
1752 pathway independent from hyphal branching. *Mycorrhiza* 1825 *Commun.* **71**, 9-18, doi:10.1107/s2053229614024929
1753 **30**, 491-501, doi:10.1007/s00572-020-00965-9 (2020). 1826 (2015).
1754 66 López-Ráez, J. A., Charnikhova, T., Gomez-Roldan, V., 1827 81 Rameau, C., Bodelin C, Cadier D, Grandjean O, Miard F &
1755 Matusova, R., Kohlen, W., De Vos, R., Verstappen, F., Puech- 1828 Murfet IC. New *ramosus* mutants at loci *Rms1*, *Rms3* and
1756 Pages, V., Becard, G., Mulder, P. & Bouwmeester, H. 1829 *Rms4* resulting from the mutation breeding program at
1757 Tomato strigolactones are derived from carotenoids and 1830 Versailles. *Pisum Genetics* **29**, 7-12 (1997).
1758 their biosynthesis is promoted by phosphate starvation. 1831 82 Braun, N., de Saint Germain, A., Pillot, J. P., Boutet-Mercey,
1759 *New Phytol.* **178**, 863-874 (2008). 1832 S., Dalmais, M., Antoniadis, I., Li, X., Maia-Gronard, A., Le
1760 67 Decker, E. L., Alder, A., Hunn, S., Ferguson, J., Lehtonen, M. 1833 Signor, C., Bouteiller, N., Luo, D., Bendahmane, A.,
1761 T., Scheler, B., Kerres, K. L., Wiedemann, G., Safavi-Rizi, V., 1834 Turnbull, C. & Rameau, C. The pea TCP transcription factor
1762 Nordzieke, S., Balakrishna, A., Baz, L., Avalos, J., Valkonen, 1835 PsBRC1 acts downstream of Strigolactones to control
1763 J. P. T., Reski, R. & Al-Babili, S. Strigolactone biosynthesis is 1836 shoot branching. *Plant Physiol.* **158**, 225-238,
1764 evolutionarily conserved, regulated by phosphate 1837 doi:10.1104/pp.111.182725 (2012).
1765 starvation and contributes to resistance against 1838 83 Cornet, F., Pillot, J.-P., Le Bris, P., Pouvreau, J.-B., Arnaud,
1766 phytopathogenic fungi in a moss, *Physcomitrella patens*. 1839 N., de Saint Germain, A. & Rameau, C. Strigolactones (SLs)
1767 *New Phytol.* **216**, 455-468, doi:10.1111/nph.14506 1840 modulate the plastochron by regulating KLUH (KLU)
1768 (2017). 1841 transcript abundance in Arabidopsis. *New Phytol.* **232**,
1769 68 Lopez-Obando, M., Guillory, A., Boyer, F.-D., Cornu, D., 1842 1909-1916, doi:10.1111/nph.17725 (2021).
1770 Hoffmann, B., Le Bris, P., Pouvreau, J.-B., Delavault, P., 1843 84 Muñoz, A., Pillot, J.-P., Cubas, P. & Rameau, C. Methods for
1771 Rameau, C., de Saint Germain, A. & Bonhomme, S. The 1844 Phenotyping Shoot Branching and Testing Strigolactone
1772 *Physcomitrium* (*Physcomitrella*) patens PpKAI2L receptors 1845 Bioactivity for Shoot Branching in Arabidopsis and Pea in
1773 for strigolactones and related compounds function via 1846 *Strigolactones: Methods and Protocols* (eds Cristina
1774 MAX2-dependent and -independent pathways. *Plant Cell* 1847 Prandi & Francesca Cardinale) 115-127 (Springer US,
1775 **33**, 3487-3512, doi:10.1093/plcell/koab217 (2021). 1848 2021). doi:10.1007/978-1-0716-1429-7_10.
1776 69 Mangnus, E. M., Dommerholt, F. J., Dejong, R. L. P. & 1849 85 Pouvreau, J.-B., Poulin, L., Huet, S. & Delavault, P.
1777 Zwanenburg, B. Improved Synthesis of Strigol Analog 1850 Strigolactone-Like Bioactivity via Parasitic Plant
1778 GR24 and Evaluation of the Biological-Activity of Its 1851 Germination Bioassay in *Strigolactones: Methods and*
1779 Diastereomers. *J. Agric. Food. Chem.* **40**, 1230-1235, 1852 *Protocols* (eds Cristina Prandi & Francesca Cardinale)
1780 doi:10.1021/jf00019a031 (1992). 1853 59-73 (Springer US, 2021). doi:10.1007/978-1-0716-
1854 1429-7_6.

1855 86 Bécard, G. & Fortin, J. A. Early events of vesicular 1863
1856 arbuscular mycorrhiza formation on Ri T-DNA 1864
1857 transformed roots. *New Phytol.* **108**, 211-218, 1865 88
1858 doi:10.1111/j.1469-8137.1988.tb03698.x (1988). 1866
1859 87 Laressergues, D., André, O., Peng, J., Wen, J., Chen, R., 1867
1860 Ratet, P., Tadege, M., Mysore, K. S. & Rochange, S. F. 1868
1861 Strigolactones contribute to shoot elongation and to the
1862 formation of leaf margin serrations in *Medicago truncatula*

R108. *J. Exp. Bot.* **66**, 1237-1244, doi:10.1093/jxb/eru471 (2015).
Fox, J. The R commander: A basic-statistics graphical user interface to R. *J. Stat. Softw.* **14**, 1-42, doi:10.18637/jss.v014.i09 (2005).

